
A NEW FRAMEWORK FOR VARIANCE-REDUCED HAMILTONIAN MONTE CARLO

A PREPRINT

Zhengmian Hu
University of Pittsburgh
Pittsburgh, PA 15213
huzhengmian@gmail.edu

Feihu Huang
University of Pittsburgh
Pittsburgh, PA 15213
huangfeihu2018@gmail.com

Heng Huang
University of Pittsburgh
Pittsburgh, PA 15213
henghuanghh@gmail.com

December 28, 2021

ABSTRACT

We propose a new framework of variance-reduced Hamiltonian Monte Carlo (HMC) methods for sampling from an L -smooth and m -strongly log-concave distribution, based on a unified formulation of biased and unbiased variance reduction methods. We study the convergence properties for HMC with gradient estimators which satisfy the Mean-Squared-Error-Bias (MSEB) property. We show that the unbiased gradient estimators, including SAGA and SVRG, based HMC methods achieve highest gradient efficiency with small batch size under high precision regime, and require $\tilde{O}(N + \kappa^2 d^{\frac{1}{2}} \varepsilon^{-1} + N^{\frac{2}{3}} \kappa^{\frac{4}{3}} d^{\frac{1}{3}} \varepsilon^{-\frac{2}{3}})$ gradient complexity to achieve ϵ -accuracy in 2-Wasserstein distance. Moreover, our HMC methods with biased gradient estimators, such as SARAH and SARGE, require $\tilde{O}(N + \sqrt{N} \kappa^2 d^{\frac{1}{2}} \varepsilon^{-1})$ gradient complexity, which has the same dependency on condition number κ and dimension d as full gradient method, but improves the dependency of sample size N for a factor of $N^{\frac{1}{2}}$. Experimental results on both synthetic and real-world benchmark data show that our new framework significantly outperforms the full gradient and stochastic gradient HMC approaches. The earliest version of this paper was submitted to ICML 2020 with three weak accept but was not finally accepted.

Keywords Variance Reduction · Sampling · Hamiltonian Monte Carlo

1 Introduction

Markov Chain Monte Carlo (MCMC) algorithms have been widely used for sampling posterior distributions in Bayesian inference. Given a dataset $\mathcal{D} = \{\mathbf{d}_i\}_{i=1}^n$, we are interested in sampling $p^*(\mathbf{x}) \propto \exp(-f(\mathbf{x}))$, where

$$f(\mathbf{x}) = -\log(p(\mathbf{x})) - \sum_{i=1}^n \log(p(\mathbf{d}_i|\mathbf{x})). \quad (1)$$

Langevin Monte Carlo (LMC) methods and Hamiltonian Monte Carlo (HMC) methods are two most popular families of gradient-based MCMC. Langevin Monte Carlo method is based on Langevin dynamics (LD) which is characterized by the following stochastic differential equation (SDE):

$$d\mathbf{X}_t = -\nabla f(\mathbf{X}_t)dt + \sqrt{2}d\mathbf{B}_t, \quad (2)$$

where \mathbf{X}_t is d -dimensional stochastic process, $t \geq 0$ denotes time, and \mathbf{B}_t is the standard d -dimensional Brownian motion. The evolution of probability distribution of \mathbf{X}_t can be addressed by the following Fokker-Planck equation:

$$\frac{\partial}{\partial t} p_t(\mathbf{x}) = \nabla^\top (p_t(\mathbf{x}) \nabla f(\mathbf{x})) + \Delta p_t(\mathbf{x}). \quad (3)$$

When the posterior distribution is well behaved [1], $p_t(\mathbf{x})$ converges to the unique stationary distribution $p^*(\mathbf{x}) \propto \exp(-f(\mathbf{x}))$. One can approximate the Langevin dynamics by applying Euler-Maruyama discretization [2] on Eq. (2),

and the corresponding update rule is given as:

$$\mathbf{x}_{k+1} = \mathbf{x}_k - \nabla f(\mathbf{x}_k)h + \sqrt{2h}\boldsymbol{\epsilon}_k, \quad (4)$$

where $\boldsymbol{\epsilon}_k$ is a d -dimensional standard Gaussian random vector, and $h > 0$ is the step size. Eq. (4) is also referred to as Unadjusted Langevin Algorithm (ULA). For strongly log-concave and log-smooth posterior distributions, [3, 4] proved that ULA converges to the target density under arbitrary precision in both total variation and 2-Wasserstein distance. The non-asymptotic convergence analysis of LMC shows that LMC algorithm can achieve ε precision in 2-Wasserstein distance after $\tilde{O}(\kappa^2 d/\varepsilon^2)$ iterations [5, 6, 7]. If additional Lipschitz continuous condition of the Hessian is satisfied, [6] showed that the dependency of convergence rate on ε can be improved to $\tilde{O}(1/\varepsilon)$. Equivalently, in order to achieve ε precision in Kullback-Leibler divergence, $\tilde{O}(\kappa^2 d/\varepsilon)$ iterations are required [8].

HMC method accelerates the convergence of LMC by Hamiltonian dynamics [9, 10]. The Hamiltonian dynamics, also known as underdamped Langevin dynamics, can explore the parameter space more efficiently by traversing along contours of a potential energy function, and can be described by the following SDE:

$$d\mathbf{X}_t = \xi \mathbf{V}_t dt, \quad d\mathbf{V}_t = -\nabla f(\mathbf{X}_t)dt - \gamma \xi \mathbf{V}_t dt + \sqrt{2\gamma} d\mathbf{B}_t, \quad (5)$$

where γ is the dissipation parameter, ξ is inverse mass, $\mathbf{X}_t, \mathbf{V}_t$ are the d -dimensional stochastic processes representing position and momentum. Under mild condition of posterior distribution, the distribution of $(\mathbf{X}_t, \mathbf{V}_t)$ converges to an unique invariant distribution $p^*(\mathbf{x}, \mathbf{v}) \propto \exp(-f(\mathbf{x}) - \frac{\xi}{2}\|\mathbf{v}\|_2^2)$, whose marginal distribution on \mathbf{X}_t coincides with posterior distribution [10]. Euler-Maruyama discretization can still be applied to Eq. (5) but that will cancel the accelerated convergence guarantees due to the low-order integration scheme. One can discretize Eq. (5) by conditioning it on the gradient at k -th iteration [11] as follows:

$$d\tilde{\mathbf{V}}_t = -\nabla f(\mathbf{x}_k)dt - \gamma \xi \tilde{\mathbf{V}}_t dt + \sqrt{2\gamma} d\mathbf{B}_t, \quad d\tilde{\mathbf{X}}_t = \xi \tilde{\mathbf{V}}_t dt. \quad (6)$$

Integration of the above SDE with a time interval h leads to the update rule of the full gradient HMC algorithm. Based on a synchronous coupling argument, [11] showed that HMC algorithm can achieve ε precision in 2-Wasserstein distance after $\tilde{O}(\kappa^2 d^{1/2}/\varepsilon)$ iterations. Under a gradient flow approach, [12] showed that, with additional Hessian Lipschitz assumption, in order to achieve ε precision in Kullback-Leibler divergence, $\tilde{O}(\kappa^{3/2} d^{1/2}/\varepsilon^{1/2})$ iterations are required.

The full gradient computation for LMC and HMC could be expensive, especially on large-scale data. Unbiased stochastic gradient estimator can be used in place of full gradient to bring down the computation requirement for each iteration. However, stochastic gradient also inevitably introduces extra variance into the sampling algorithm at each step which impedes the convergence. [5, 6] studied Stochastic Gradient Langevin Dynamics (SGLD) [13] and showed that the gradient complexity of SGLD is $\tilde{O}(\kappa^2 d\sigma^2/\varepsilon^2)$, where ε is accuracy in 2-Wasserstein distance, and σ^2 is the upper bound of the variance of the stochastic gradient. Unlike the full gradient case, assuming extra Hessian smoothness can not improve the dependence of convergence rate on ε further. Stochastic Gradient Hamiltonian Monte Carlo (SG-HMC) was studied in [11, 14, 15]. [11] proved the gradient complexity of SG-HMC as $\tilde{O}(\kappa^2 d\sigma^2/\varepsilon^2)$, which is $\tilde{O}(\frac{d^{1/2}\sigma^2}{N\varepsilon})$ worse than the full gradient HMC in 2-Wasserstein distance. In both SGLD and SG-HMC, the gradient complexity is dominated by the variance of the stochastic gradient.

Since the potential energy function normally can be decomposed as finite sum of smooth functions as in Eq. (1), variance reduction technique can be employed to reduce the variance of stochastic gradient. Dubey et al. [16] and Li et al. [17] studied variance reduced LMC and HMC, respectively. They showed that SAGA and SVRG reduce the mean square error (MSE) of the sample path for some test functions, but did not provide gradient complexity with respect to any divergence. Baker et al. [18] studied the control-variate technique applied to stochastic gradient Langevin dynamics. Although the convergence rate of control-variate SGLD is no longer dominated by the gradient variance σ^2 , the dependency on ε is still worse than full gradient method. Chatterji et al. [19] studied control-variate underdamped Langevin dynamics (CV-ULD) but their analysis showed that CV-ULD is not guaranteed to converge to arbitrary precision. With Hessian Lipschitz assumption, Chatterji et al. [19] proved two sharper convergence rates for SAGA and SVRG based LMC, which recovers the convergence rate of full gradient method under 2-Wasserstein metric in terms of dependence on the sampling accuracy ε . Zou et al. [20] analyzed SVRG based HMC with fixed batch size $b = 1$, however for a fixed step size, the algorithm is not guaranteed to converge after an arbitrary number of steps.

In addition to variance reduction, there are other branches of research that can improve HMC. Symplectic integration schemes including leapfrog methods leverage symplecticity of canonical transformation and achieve better dependency on d [21]. Replica exchange [22, 23] allows exploring the multi-mode landscape more efficiently. However, these techniques are orthogonal to the research direction of our framework and is of independent interest.

In this paper, we propose a new framework of variance-reduced Hamiltonian Monte Carlo method to leverage most popular variance reduction techniques, including SAGA [24], SVRG [25], SARAH [26], and SARGE [27]. Our

Methods	Reference	Batch size	Gradient complexity	Converge at Infinite Time
HMC	[11]	N	$\tilde{O}(N\kappa^2 d^{\frac{1}{2}}/\varepsilon)$	Y
SG-HMC	[11]	$O(1)$	$\tilde{O}(\kappa^2 \sigma^2 d/\varepsilon^2)$	Y
SVRG-HMC	[20]	1	$\tilde{O}(N + \kappa^2 d^{\frac{1}{2}}/\varepsilon + N^{\frac{2}{3}} \kappa^{\frac{3}{4}} d^{\frac{1}{3}}/\varepsilon^{\frac{2}{3}})$	N
SVRG-HMC	Ours	1	$\tilde{O}(N\kappa^2 + \kappa^2 d^{\frac{1}{2}}/\varepsilon + N^{\frac{2}{3}} \kappa^{\frac{3}{4}} d^{\frac{1}{3}}/\varepsilon^{\frac{2}{3}})$	Y
SAGA-HMC	Ours	1	$\tilde{O}(N\kappa^2 + \kappa^2 d^{\frac{1}{2}}/\varepsilon + N^{\frac{2}{3}} \kappa^{\frac{3}{4}} d^{\frac{1}{3}}/\varepsilon^{\frac{2}{3}})$	Y
SVRG-HMC	Ours	b	$\tilde{O}(N + N\kappa^2/b^{\frac{1}{2}} + b\kappa^2 d^{\frac{1}{2}}/\varepsilon + N^{\frac{2}{3}} \kappa^{\frac{3}{4}} d^{\frac{1}{3}}/\varepsilon^{\frac{2}{3}})$	Y
SAGA-HMC	Ours	b	$\tilde{O}(N + N\kappa^2/b^{\frac{1}{2}} + b\kappa^2 d^{\frac{1}{2}}/\varepsilon + N^{\frac{2}{3}} \kappa^{\frac{3}{4}} d^{\frac{1}{3}}/\varepsilon^{\frac{2}{3}})$	Y
SARAH-HMC	Ours	1	$\tilde{O}(N + N^{\frac{1}{2}} \kappa^2 d^{\frac{1}{2}}/\varepsilon)$	Y
SARGE-HMC	Ours	1	$\tilde{O}(N + N^{\frac{1}{2}} \kappa^2 d^{\frac{1}{2}}/\varepsilon)$	Y

Table 1: Gradient complexity of different Hamiltonian Monte Carlo methods for sampling L -smooth and m -strongly log-concave distribution. We accept the large mini-batch size $b > 1$.

algorithm was inspired by the recent advance in stochastic optimization [27], which depicts semi-stochastic gradients with so called MSEB property to control the MSE and bias.

To show the advantages of our new methods, we summarize and compare the gradient computational complexity for different Hamiltonian Monte Carlo methods in Table 1. In Table 1, ε represents the accuracy under 2-Wasserstein distance, N is the sample size, b denotes batch size, and all average epoch lengths for SARAH and SVRG are set as $p = O(N/b)$. Our main contributions in this paper can be summarized as follows:

1. We propose a new Hamiltonian Monte Carlo framework to leverage popular variance reduction techniques, including both biased and unbiased gradient estimators.
2. In theoretical analysis, we prove the convergence of our framework with MSEB estimator in a general manner. As a specialization, we consider four variance-reduced gradient estimators, SAGA, SVRG, SARAH, and SARGE, and derive the convergence rate under 2-Wasserstein metric for them. All variance reduction methods considered in this paper enjoy better convergence rate than existing full gradient method and stochastic gradient methods.
3. To the best of our knowledge, the biased variance reduction techniques, including SARAH and SARGE, have not been incorporated into stochastic HMC for sampling strongly-log-concave distribution, and this paper provides the first convergence result for them.

2 Preliminary

In order to show the convergence of our variance reduced HMC framework for sampling from an L -smooth and m -strongly log-concave distribution $p^* \propto e^{-f(x)}$, we need to introduce some mild assumptions on the potential energy function $f(x) : \mathbb{R}^d \rightarrow \mathbb{R}$ as follows:

Assumption 1 (Sum-decomposable). $f(x) = \sum_{i=1}^N f_i(x)$, where integer N is the sample size.

Assumption 2 (Smoothness). Each function f_i is continuously-differentiable on \mathbb{R}^d and there exists a constant $\tilde{L} > 0$, such that

$$\|\nabla f_i(\mathbf{x}) - \nabla f_i(\mathbf{y})\|_2 \leq \tilde{L} \|\mathbf{x} - \mathbf{y}\|_2$$

for any $\mathbf{x}, \mathbf{y} \in \mathbb{R}^d$. It can be easily verified that $f(x)$ is L -smooth with $L = N\tilde{L}$.

Assumption 3 (Strong Convexity). There exists a constant $m > 0$ such that

$$f(\mathbf{x}) - f(\mathbf{y}) \geq \langle \nabla f(\mathbf{y}), \mathbf{x} - \mathbf{y} \rangle + \frac{m}{2} \|\mathbf{x} - \mathbf{y}\|_2^2.$$

We define the condition number $\kappa := L/m$.

Assumption 4 (Optimal at Zero). Without loss of generality, we assume $\mathbf{x}^* = 0$ and $f(\mathbf{x}^*) = 0$ where \mathbf{x}^* is the global minimizer for the strongly convex potential energy function.

Wasserstein Distance: Given a pair of probability measures μ and ν , we define a transference plan ζ between μ and ν as a joint distributions such that marginal distribution of the first set of coordinates is μ and marginal distribution of

the second set of coordinates is ν . We denote $\Gamma(\mu, \nu)$ as the set of all transference plans. We define the 2-Wasserstein distance between μ and ν as follows,

$$W_2^2(\mu, \nu) = \inf_{\zeta \in \Gamma(\mu, \nu)} \int \|\mathbf{x} - \mathbf{y}\|_2^2 d\zeta(x, y).$$

MSEB property: Given a parameter sequence $\{\mathbf{x}_k\}$ and a function f , a stochastic gradient estimator $\tilde{\nabla}$ is a series of vectors $\tilde{\nabla}_k$ generated from $\{\mathbf{x}_i\}_{i=0}^k$. We say that a stochastic gradient estimator $\tilde{\nabla}$ satisfies MSEB property if there exist constants $M_1, M_2 \geq 0, \rho_M, \rho_B, \rho_F \in (0, 1]$ and sequences \mathcal{M}_k and \mathcal{F}_k such that

$$\begin{aligned} \nabla f((x_{k+1})) - \mathbb{E}_k \tilde{\nabla}_{k+1} &= (1 - \rho_B)(\nabla f((x_k)) - \tilde{\nabla}_k) \\ \mathbb{E} \left\| \tilde{\nabla}_{k+1} - \nabla f(\mathbf{x}_{k+1}) \right\|_2^2 &\leq \mathcal{M}_k \\ \mathcal{M}_k &\leq M_1 Q_k + \mathcal{F}_k + (1 - \rho_M) \mathcal{M}_{k-1} \\ \mathcal{F}_k &\leq \sum_{l=0}^k M_2 (1 - \rho_F)^{k-l} Q_l \\ Q_k &= N \sum_{i=1}^N \mathbb{E} \left\| \nabla f_i(\mathbf{x}_{k+1}) - \nabla f_i(\mathbf{x}_k) \right\|_2^2. \end{aligned} \tag{7}$$

\mathbb{E}_k means expectation conditioned on all variables at k -th step and all previous steps. MSEB property controls the bias and MSE of the gradient estimator with a weighted sum of gradient changes $\|\nabla f_i((x_{k+1})) - \nabla f_i((x_k))\|_2^2$ along the previous sample path. Note that many popular gradient estimators including SAGA [24], SVRG [25], SARAH [26], and SARGE [27] satisfy MSEB property.

3 A New Framework for Variance-Reduced Hamiltonian Monte Carlo

In the section, we propose a new framework for variance-reduced Hamiltonian Monte Carlo based on the MSEB property.

We first derive the update rule by integrating the SDE of Hamiltonian dynamics Eq. (6). With step as h , we obtain the following update rule:

$$\begin{aligned} \mathbf{x}_{k+1} &= \tilde{\mathbf{X}}_h = \mathbf{x}_k + \frac{1}{\gamma} (1 - e^{-\gamma \xi h}) \mathbf{v}_k \\ &\quad - \frac{1}{\gamma} \left(h - \frac{1}{\gamma \xi} (1 - e^{-\gamma \xi h}) \right) \nabla f(\mathbf{x}_k) + \mathbf{e}_k^x, \\ \mathbf{v}_{k+1} &= \tilde{\mathbf{V}}_h = e^{-\gamma \xi h} \mathbf{v}_k - \frac{1}{\gamma \xi} (1 - e^{-\gamma \xi h}) \nabla f(\mathbf{x}_k) + \mathbf{e}_k^v, \end{aligned} \tag{8}$$

where \mathbf{e}_k^v and \mathbf{e}_k^x denote Gaussian random vectors with zero mean and the following covariance:

$$\begin{aligned} \mathbb{E}(\mathbf{e}_k^v \mathbf{e}_k^{v\top}) &= \frac{1}{\xi} (1 - e^{-2\gamma \xi h}) \mathbf{I}_{d \times d} \\ \mathbb{E}(\mathbf{e}_k^x \mathbf{e}_k^{v\top}) &= \frac{1}{\gamma \xi} (1 + e^{-2\gamma \xi h} - 2e^{-\gamma \xi h}) \mathbf{I}_{d \times d} \\ \mathbb{E}(\mathbf{e}_k^x \mathbf{e}_k^{x\top}) &= \frac{1}{\gamma^2 \xi} (2\gamma \xi h - 3 + 4e^{-\gamma \xi h} - e^{-2\gamma \xi h}) \mathbf{I}_{d \times d} \end{aligned} \tag{9}$$

For the sum decomposable function $f(\mathbf{x}) = \sum_{i=1}^N f_i(\mathbf{x})$, the stochastic gradient can be used to reduce the computation for single iteration by substituting full gradient $\nabla f(\mathbf{x}_k)$ with stochastic gradient $\frac{N}{|\mathcal{B}_k|} \sum_{i \in \mathcal{B}_k} \nabla f_i(\mathbf{x}_k)$. However the gradient error of stochastic gradient can be large and hinders the convergence. Variance reduction techniques could remedy this problem by using historical gradient information to reduce the gradient error of current iterate. The idea of variance reduction has been widely used in optimization and there exist many popular choices for variance reduction techniques such as SAGA, SVRG, SARGE and SARAH.

In order to leverage the advances of different variance reduction methods to accelerate HMC, we use MSEB property to deal with different variance reduction methods uniformly, and propose a framework that is compatible with all MSEB gradient estimators. Our framework is summarized in Algorithm 1. Now we can state the convergence guarantee for our variance reduced HMC framework.

Theorem 1. *Let f be a function satisfying Assumptions 1 to 4, $\tilde{\nabla}_k$ is an MSEB estimator. Let the initial point be $(\mathbf{x}_0, 0)$ and the initial distribution be $p_0(\mathbf{x}, \mathbf{v}) = \delta_{\mathbf{x}=\mathbf{x}_0} \delta_{\mathbf{v}=0}$. With small enough step size h satisfying $Lh \leq \frac{1}{10\kappa} \min(1, \frac{1}{\sqrt{\Theta}})$,*

Algorithm 1: Variance-Reduced HMC (VR-HMC) Algorithm

Input: Initial point $(\mathbf{x}_0, \mathbf{v}_0)$, smoothness parameter L and step size $h > 0$.
for $k = 0$ **to** $K - 1$ **do**
 Generate the variance reduced stochastic gradient $\tilde{\nabla}_k$ which satisfied MSEB property;
 Generate Gaussian random vectors \mathbf{e}_k^x and \mathbf{e}_k^v based with covariance in (9);
 Update $\mathbf{x}_{k+1} = \mathbf{x}_k + \frac{1}{\gamma}(1 - e^{-\gamma\xi h})\mathbf{v}_k - \frac{1}{\gamma}(h - \frac{1}{\gamma\xi}(1 - e^{-\gamma\xi h}))\tilde{\nabla}_k + \mathbf{e}_k^x$;
 Update $\mathbf{v}_{k+1} = e^{-\gamma\xi h}\mathbf{v}_k - \frac{1}{\gamma\xi}(1 - e^{-\gamma\xi h})\tilde{\nabla}_k + \mathbf{e}_k^v$.
end for
Output: \mathbf{v}_K .

denoting $q_k = (\mathbf{x}_k, \mathbf{x}_k + \mathbf{v}_k)$, after running the Algorithm 1 for k iterations, we have:

$$W_2(q_k, q^*) \leq e^{-\frac{k h m}{2}} W_2(q_0, q^*) + 8\sqrt{L F_2 \kappa} h + 4\sqrt{\Theta F_1} \left(2(1 - \rho_B)\sqrt{L \kappa} h + L\sqrt{\kappa} h^{\frac{3}{2}} \right),$$

where $p^*(\mathbf{x}, \mathbf{v}) = q^*(\mathbf{x}, \mathbf{x} + \mathbf{v}) \propto \exp(-f(\mathbf{x}) - \frac{\xi}{2}\|\mathbf{v}\|_2^2)$, $\Theta = \frac{M_1}{\rho_M} + \frac{M_2}{\rho_M \rho_F}$, $F_1 = 13L\|\mathbf{x}_0\|_2^2 + 24\kappa d$ and $F_2 = 97L\|\mathbf{x}_0\|_2^2 + 181\kappa d$.

Corollary 1. For unbiased gradient estimator, we have $\rho_B = 1$. Under the same conditions as in Theorem 1, let the step size be

$$Lh \leq \min(\varepsilon \kappa^{-\frac{3}{2}} L^{\frac{1}{2}} d^{-\frac{1}{2}}, \varepsilon^{\frac{2}{3}} \kappa^{-\frac{2}{3}} L^{\frac{1}{3}} d^{-\frac{1}{3}}, \frac{1}{10\kappa \max(1, \sqrt{\Theta})}).$$

The output of Algorithm 1 with unbiased gradient estimator satisfies $W_2(q_k, q^*) \leq \varepsilon$, within $\tilde{O}(\sqrt{\Theta} \kappa^2 + \kappa^2 d^{\frac{1}{2}} \varepsilon^{-1} + \Theta^{\frac{1}{3}} \kappa^{\frac{4}{3}} d^{\frac{1}{3}} \varepsilon^{-\frac{2}{3}})$ iterations.

Remark 1. The first term $\sqrt{\Theta} \kappa^2$ in the iteration complexity comes from the restriction of small step size $Lh \leq \frac{1}{10\kappa \sqrt{\Theta}}$ and is independent of precision ε . If we assume high precision condition $\varepsilon \leq \frac{d^{\frac{1}{2}}}{\min(\sqrt{\Theta}, \kappa \Theta^{\frac{1}{4}})}$, the first term is dominated by the second or third term thus the iteration complexity would be $\tilde{O}(\kappa^2 d^{\frac{1}{2}} \varepsilon^{-1} + \Theta^{\frac{1}{3}} \kappa^{\frac{4}{3}} d^{\frac{1}{3}} \varepsilon^{-\frac{2}{3}})$. The restriction of small step size is necessary for the convergence after running the algorithm for arbitrary long time. We notice that [20] didn't assume small step size. As a result, they can only guarantee the convergence for $k < O(\frac{1}{L^2 h^2 \kappa})$.

Corollary 2. For biased gradient estimator, we have $\rho_B < 1$. Under the same conditions as in Theorem 1, for precision $\varepsilon > 0$, let the step size satisfy

$$Lh \leq \varepsilon \kappa^{-\frac{3}{2}} L^{\frac{1}{2}} d^{-\frac{1}{2}} \min(1, \frac{1}{\sqrt{\Theta}}).$$

The output distribution of Algorithm 1 with biased gradient estimator satisfies $W_2(q_k, q^*) \leq \varepsilon$, within $\tilde{O}((1 + \sqrt{\Theta}) \kappa^2 d^{\frac{1}{2}} \varepsilon^{-1})$ iterations.

Remark 2. Recall that the iteration complexity of SG-HMC is $\tilde{O}(\kappa^2 d \sigma^2 / \varepsilon^2)$ [11]. Compared to SG-HMC, both biased and unbiased variance-reduced HMC improve the dependency of ε . Compared to the convergence rate $\tilde{O}(\kappa^2 d^{\frac{1}{2}} / \varepsilon)$ of full gradient HMC [11], our algorithm with unbiased gradient estimator is penalized by a term $\Theta^{\frac{1}{3}} \kappa^{\frac{4}{3}} d^{\frac{1}{3}} \varepsilon^{-\frac{2}{3}}$, and our algorithm with biased gradient estimator is penalized by a factor of $O(1 + \sqrt{\Theta})$. Therefore, our methods with MSEB gradient estimator takes more iterations than full gradient HMC to achieve same accuracy. This regression comes from the perturbation of inaccurate gradient estimator and is controlled by parameter Θ .

3.1 Convergence Properties for Specific Estimators

Under Theorem 1, we can prove the convergence rate of a specific gradient estimator for Algorithm 1 by just establishing bounds on the MSEB terms in (7).

We first consider full gradient as a special case of MSEB gradient estimator where no bias or mean square error exists.

Corollary 3 (Full Gradient). When we use full gradient in Algorithm 1, $\Theta = 0$, we need $\tilde{O}(\kappa^2 d^{\frac{1}{2}} / \varepsilon)$ iterations to achieve ε accuracy in 2-Wasserstein distance. Given that computing a full gradient requires N queries on the gradient of each component function $f_i(\mathbf{x})$, we can show the gradient complexity is $\tilde{O}(N \kappa^2 d^{\frac{1}{2}} / \varepsilon)$.

Remark 3. Recall that previous research [11] has shown that the gradient complexity of full gradient HMC is $\tilde{O}(N\kappa^2 d^{\frac{1}{2}}/\varepsilon)$. Our result can successfully achieve such gradient complexity, which implies that our analysis is tight under the notation of MSEB estimator.

Next we combine unbiased variance reduction methods with our framework to improve the gradient complexity. We choose two most popular unbiased variance reduction methods SVRG and SAGA.

SVRG was first proposed for strongly convex optimization in [25] as an unbiased variance reduction technique to accelerate the convergence to the global minimizer. The estimated gradient is calculated in the following way where B_k is the batch of k -th iteration:

$$\tilde{\nabla}_k^{SVRG} = \frac{N}{b} \sum_{i \in B_k} (\nabla f_i(\mathbf{x}_k) - \nabla f_i(\tilde{\mathbf{x}})) + \nabla f(\tilde{\mathbf{x}}).$$

SVRG updates the snapshot $\tilde{\mathbf{x}}$ periodically and computes the full gradient $\nabla f(\tilde{\mathbf{x}})$ on the snapshot. Despite extra gradient queries, it was shown that SVRG has lower gradient MSE and enjoys better gradient complexity under many setting of optimization.

The original SVRG has an inner and outer loop structure which is not compatible with our framework. In order to combine it with MSEB property, we consider a variant of SVRG where the snapshot is updated with probability $\frac{1}{p}$ at each iteration, such that the average interval between snapshot updates is p iterations.

SAGA [24] is another popular variance-reduced algorithm. Instead of calculating the full gradient of a previous snapshot, the most recent gradient information ϕ_k^i of each component function $f_i(\mathbf{x})$ is stored. SAGA estimates the gradient as follows:

$$\tilde{\nabla}_k^{SAGA} = \frac{N}{b} \sum_{i \in B_k} (\phi_k^i - \phi_{k-1}^i) + \sum_{i=1}^N \phi_{k-1}^i.$$

The most recent gradient ϕ_k^i is set as $\nabla f_i(\mathbf{x}_k)$ if the component functions f_i is in the batch of k -th iteration, otherwise it remains the same as ϕ_{k-1}^i . SAGA avoids the extra gradient computation compared with SVRG, however, it requires much more memory to store the old gradient information for each data point.

SAGA and SVRG are both unbiased gradient estimators since $\mathbb{E}_k \tilde{\nabla}_{k+1} = \nabla f(\mathbf{x}_{k+1})$. According to Corollary 1, we can obtain the gradient complexity by just studying the MSEB terms.

Corollary 4 (SVRG). When SVRG is used in Algorithm 1, let b be the batch size, p be the average number of iterations between snapshot updates, and we have $\Theta = \frac{6p^2}{b}$, and for each iteration, $N/p + 2b$ gradient queries are needed in average. The gradient complexity is $\tilde{O}(N + (N/b^{\frac{1}{2}} + pb^{\frac{1}{2}})\kappa^2 + b\kappa^2 d^{\frac{1}{2}}/\varepsilon + (N/(pb)^{\frac{1}{3}} + (pb)^{\frac{2}{3}})\kappa^{\frac{4}{3}} d^{\frac{1}{3}}/\varepsilon^{\frac{2}{3}})$. Most of the time, we choose $p = O(N/b)$, then the gradient complexity is $\tilde{O}(N + N\kappa^2/b^{\frac{1}{2}} + b\kappa^2 d^{\frac{1}{2}}/\varepsilon + N^{\frac{2}{3}}\kappa^{\frac{4}{3}} d^{\frac{1}{3}}/\varepsilon^{\frac{2}{3}})$. Let the batch size be $b = 1$, the gradient complexity is $\tilde{O}(N\kappa^2 + \kappa^2 d^{\frac{1}{2}}/\varepsilon + N^{\frac{2}{3}}\kappa^{\frac{4}{3}} d^{\frac{1}{3}}/\varepsilon^{\frac{2}{3}})$.

Corollary 5 (SAGA). When SAGA is used in Algorithm 1, let b be the batch size, and we have $\Theta = \frac{6N^2}{b^3}$, and the gradient complexity is $\tilde{O}(N + N\kappa^2/b^{\frac{1}{2}} + b\kappa^2 d^{\frac{1}{2}}/\varepsilon + N^{\frac{2}{3}}\kappa^{\frac{4}{3}} d^{\frac{1}{3}}/\varepsilon^{\frac{2}{3}})$. Let the batch size be $b = 1$, the gradient complexity is $\tilde{O}(N\kappa^2 + \kappa^2 d^{\frac{1}{2}}/\varepsilon + N^{\frac{2}{3}}\kappa^{\frac{4}{3}} d^{\frac{1}{3}}/\varepsilon^{\frac{2}{3}})$.

If we set $p = N/b$ for SVRG, both SAGA and SVRG have the same Θ , which means they have similar effect on reducing the variance of the gradient estimation. As a result, our HMC framework with these two techniques have same gradient complexity $\tilde{O}(N + N\kappa^2/b^{\frac{1}{2}} + b\kappa^2 d^{\frac{1}{2}}/\varepsilon + N^{\frac{2}{3}}\kappa^{\frac{4}{3}} d^{\frac{1}{3}}/\varepsilon^{\frac{2}{3}})$.

Each term in the above gradient complexity is strictly better than the gradient complexity $\tilde{O}(N\kappa^2 d^{\frac{1}{2}}/\varepsilon)$ of full gradient method. Compared with the gradient complexity of stochastic gradient HMC $\tilde{O}(\kappa^2 d \sigma^2/\varepsilon^2)$, where we assume $\mathbb{E} \|\nabla f_i(\mathbf{x}) - \nabla f(\mathbf{x})\|_2^2 \leq \sigma^2$, our result has better dependency on d and ε , and our analysis doesn't depend on extra assumption on the bounded variance of stochastic gradient.

We further discuss the choice strategy of the batch size under different regimes:

1. Under low precision regime, $\varepsilon \geq \frac{d^{\frac{1}{2}}}{\min(\sqrt{\Theta}, \kappa \Theta^{\frac{1}{4}})} = \max(\frac{d^{\frac{1}{2}} b^{\frac{3}{2}}}{N}, \frac{d^{\frac{1}{2}} b^{\frac{3}{4}}}{N^{\frac{1}{2}} \kappa})$, the last two terms that are ε dependent are dominated by the second term. Therefore the gradient complexity is $\tilde{O}(N + N\kappa^2/b^{\frac{1}{2}})$. Clearly in this regime, increasing the batch size could help decrease the gradient complexity.

Methods	HMC	SG-HMC	SVRG-HMC	SARAH-HMC	SAGA-HMC	SARGE-HMC
Potential MSE ($\times 10^{-5}$)	19 ± 3	1187 ± 30	19 ± 3	19 ± 3	21 ± 3	356 ± 17
Gradient MSE	0.0	845.549 ± 0.022	0.0	0.0	21.146 ± 0.005	1.1042 ± 0.0003

Table 2: Potential energy MSE and gradient MSE for different Hamiltonian Monte Carlo Methods on synthetic data.

2. Under high precision regime, $\varepsilon \leq \max(\frac{d^{\frac{1}{2}}b^{\frac{3}{2}}}{N}, \frac{d^{\frac{1}{2}}b^{\frac{3}{4}}}{N^{\frac{1}{2}}\kappa})$, the gradient complexity changes to $\tilde{O}(N + b\kappa^2d^{\frac{1}{2}}/\varepsilon + N^{\frac{2}{3}}\kappa^{\frac{4}{3}}d^{\frac{1}{3}}/\varepsilon^{\frac{2}{3}})$. This result encourage us to decrease the batch size when the term $b\kappa^2d^{\frac{1}{2}}/\varepsilon$ is dominant.
3. Under high precision regime, if we further assume $\varepsilon \geq \frac{b^3\kappa^2d}{N^2}$, then the last term dominates the second and third terms. The gradient complexity changes to $\tilde{O}(N + N^{\frac{2}{3}}\kappa^{\frac{4}{3}}d^{\frac{1}{3}}/\varepsilon^{\frac{2}{3}})$ and is independent of batch size b . Therefore, we can increase the batch to as large as $\frac{\varepsilon^{\frac{1}{3}}N^{\frac{2}{3}}}{\kappa^{\frac{4}{3}}d^{\frac{1}{3}}}$ without hurting the convergence rate.
4. Under high precision regime, if we assume $\varepsilon \leq \frac{b^3\kappa^2d}{N^2}$, the gradient complexity changes to $\tilde{O}(N + b\kappa^2d^{\frac{1}{2}}/\varepsilon)$, which is positively correlated with batch size b . If $\varepsilon \leq \min(\frac{\kappa^2d}{N^2}, \frac{d^{\frac{1}{2}}}{N})$ the best gradient complexity is achieved by setting $b = 1$.

Biased stochastic gradient methods were not wildly adopted in previous sampling methods because of the difficulties in the algorithm convergence guarantee and theoretical analysis. We show that the biased estimators can still be applied together with our HMC framework for sampling strongly-log-concave distribution to achieve acceleration. However, the bias might outweigh the benefits of a lower gradient MSE and hurt the convergence rate. In this paper, we consider SARAH and SARGE because they can further reduce the MSE of the gradient estimation.

SARAH [26] is very similar to SVRG but estimates the full gradient in a recursive way:

$$\tilde{\nabla}_k^{SARAH} = \frac{N}{b} \sum_{i \in B_k} (\nabla f_i(\mathbf{x}_k) - \nabla f_i(\mathbf{x}_{k-1})) + \tilde{\nabla}_{k-1}^{SARAH}$$

SARAH also needs to reset gradient estimator $\tilde{\nabla}_k^{SARAH}$ to full gradient $\nabla f(\mathbf{x}_k)$ periodically, which leads to inner and outer loop structure in the algorithm. In order to prove the MSEB property for SARAH, we consider a variant of SARAH where the full gradient is calculated with probability $\frac{1}{p}$ at each iteration.

SARGE [27] doesn't require computing the full gradient repeatedly but requires the extra storage. The gradient is estimated as follows:

$$\tilde{\nabla}_k^{SARGE} = \frac{N}{b} \sum_{i \in B_k} (\psi_k^i - \psi_{k-1}^i) + \sum_{i=1}^N \psi_{k-1}^i + (1 - \frac{b}{N})\tilde{\nabla}_{k-1}^{SARGE}$$

where ψ_k^i is updated as $\nabla f_i(\mathbf{x}_k) - (1 - \frac{b}{N})\nabla f_i(\mathbf{x}_{k-1})$ if i is in the batch, otherwise remains the same.

We then deduce the convergence guarantee for our framework based on SARAH and SARGE.

Corollary 6 (SARAH). *When using SARAH in Algorithm 1, let b be the batch size, p be the average number of iterations between calculating full gradient, we have $\Theta = p$ and $\rho_B = \frac{1}{p}$, and the gradient complexity is $\tilde{O}(N + (b + bp^{\frac{1}{2}})\kappa^2d^{\frac{1}{2}}/\varepsilon)$. Let the batch size be $b = 1$, and the average interval between full gradient updates be $p = O(N/b)$, the gradient complexity is $\tilde{O}(N + N^{\frac{1}{2}}\kappa^2d^{\frac{1}{2}}/\varepsilon)$.*

Corollary 7 (SARGE). *When using SVRG in Algorithm 1, let b be the batch size, we have $\Theta = \frac{72N}{b} + \frac{108N}{b^2}$ and $\rho_B = \frac{b}{N}$, and the gradient complexity is $\tilde{O}(N + (b + N^{\frac{1}{2}}b^{\frac{1}{2}})\kappa^2d^{\frac{1}{2}}/\varepsilon)$. Let the batch size be $b = 1$, the gradient complexity is $\tilde{O}(N + N^{\frac{1}{2}}\kappa^2d^{\frac{1}{2}}/\varepsilon)$.*

Both SARAH and SARGE achieve their best gradient complexity of $\tilde{O}(N + N^{\frac{1}{2}}\kappa^2d^{\frac{1}{2}}/\varepsilon)$ with small batch $b = 1$. Compared with full gradient methods, the dependency of dataset size N is improved by a factor $N^{\frac{1}{2}}$. If compared with stochastic gradient methods, the dependency of ε is improved by a factor of $1/\varepsilon$.

Compared with SAGA and SVRG, SARAH and SARGE have much smaller gradient MSE since Θ has better dependency of N . However, this comes with the price of non-zero gradient bias, which hurts the convergence rate in dependency of ε . Therefore, in the high precision regime, HMC with biased gradient estimator could converge slower than HMC with unbiased gradient estimators even if with smaller gradient MSE.

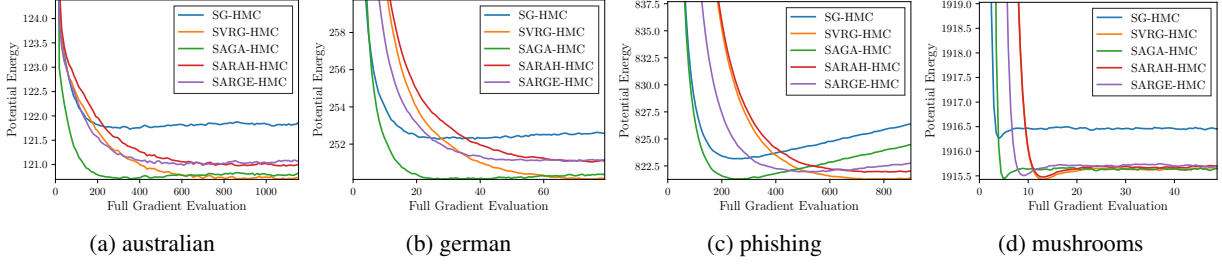


Figure 1: Mean potential energy of different algorithms on training datasets for logistic regression task.

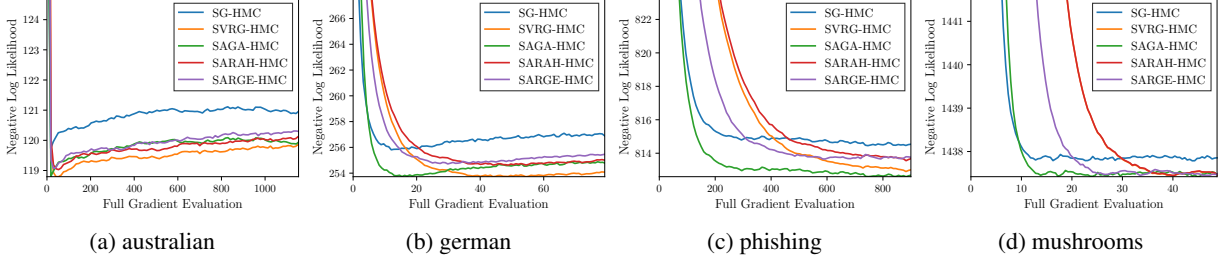


Figure 2: Negative log-likelihood energy of different algorithms on testing datasets for logistic regression task.

4 Experimental Results

In this section, we will evaluate our algorithms on both synthetic data and real-world benchmark data. During the following experiments, SVRG, SAGA, SARAH, and SARGE will be incorporated with our framework for evaluations. The corresponding algorithms are called as SVRG-HMC, SAGA-HMC, SARAH-HMC, and SARGE-HMC, respectively.

4.1 Synthetic Data

Following previous works [15, 20], we use quadratic function as potential energy for our synthetic data. The potential energy function can be decomposed into N components $f_i(\mathbf{x}) = \frac{1}{N}(\mathbf{d}_i - \mathbf{x})^\top \Sigma^{-1}(\mathbf{d}_i - \mathbf{x})$, where $\mathbf{x} \in \mathbb{R}^d$ is the parameter to sample and $\mathbf{d}_i \in \mathbb{R}^d$ is the i -th data element generated from $\mathbf{d}_i \sim \mathcal{N}(\mathbf{2}, 2\mathbf{I}_{d \times d})$. Σ^{-1} is a random positive-definite matrix whose maximum eigenvalue is L and the minimum eigenvalue is m . Clearly, the invariant distribution is a Gaussian distribution with mean as average of \mathbf{d}_i and covariance as Σ . During the experiment, we set $L = 10, d = 5, N = 1000$.

We set uniform step size for different algorithms and set batch size as $b = 1$. We estimate the mean potential energy by accumulating for ten million iterations after burn-in of ten thousand iterations. We report the MSE of mean potential energy and gradient MSE of different algorithms in Table 2.

Firstly, all variance reduction methods based HMC enjoy more accurate gradient estimation and have smaller sampling error than SG-HMC. Due to the simpleness of the quadratic potential function, SVRG and SARGE can eliminate the gradient error, thus the sampling error of SVRG-HMC and SARGE-HMC is exactly the same as full gradient HMC. We also notice that SARGE-HMC achieves smaller gradient error than SAGA-HMC, but has larger MSE on potential energy. This supports our theoretical analysis: the biased gradient estimator based HMC could be worse than the unbiased one even if with smaller gradient MSE.

Table 3: The summary of different datasets used in our experiments.

Dataset	australian	german	phishing	mushrooms
N	690	1000	11055	8124
d	14	24	68	112

4.2 Bayesian Logistic Regression

We further conduct experiments in Bayesian Logistic Regression on multiple real-world benchmark datasets.

Typically in logistic regression, we are given a group of pairs $\{\mathbf{a}_i, y_i\}$, where \mathbf{a}_i is the feature vector and y_i is binary label for each sample. We assume the likelihood function has the form $p(y_i|\mathbf{a}_i, \mathbf{x}) = \frac{1}{1+\exp(-y_i \mathbf{a}_i^\top \mathbf{x})}$, then we have the

posterior of parameter \mathbf{x} as: $p^*(\mathbf{x}) = p_{prior}(\mathbf{x}) \prod_{i=1}^N p(y_i|\mathbf{a}_i, \mathbf{x})$.

Here we use the Gaussian distribution $\mathcal{N}(\mathbf{0}, m^{-1} \mathbf{I}_{d \times d})$ as prior. The corresponding potential energy function $f(\mathbf{x})$ can be written as:

$$f(\mathbf{x}) = \frac{m}{2} \|\mathbf{x}\|_2^2 + \sum_{i=1}^N \log(1 + \exp(-y_i \mathbf{a}_i^\top \mathbf{x})).$$

We choose four benchmark datasets from LIBSVM [28]. Their dimensionality and sample size are summarized in Table 3. We divide the data into training set and testing set evenly. The batch size is set to 1 for all algorithms. Since it is computationally intractable to calculate the 2-Wasserstein distance in high dimensional space, we choose to record the average potential energy for training dataset and negative log-likelihood for testing dataset along the sample path to reflect the convergence and sampling error. In order to control the influence of step size on the sampling error, we choose a uniform step size for all algorithms. We also set small batch size $b = 1$ for all algorithms. We run each algorithm several thousand times and report the average result to reduce the noise. The full gradient method is not examined due to slow convergence. The potential energy for training dataset is shown in Figure 1 and the negative log-likelihood for testing dataset is shown in Figure 2.

Obviously all variance reduced methods based HMC achieve lower mean potential energy compared to the SG-HMC, which indicates that our HMC framework can approximate the posterior much better than SG-HMC. We also notice that all algorithms take similar number of iterations to reach equilibrium. However, SVRG-HMC and SARAH-HMC take three gradient queries for each iteration on average and SARGE-HMC takes two gradient queries for each iteration. Therefore, these methods need more gradient evaluation for burn-in than SAGA-HMC and SG-HMC.

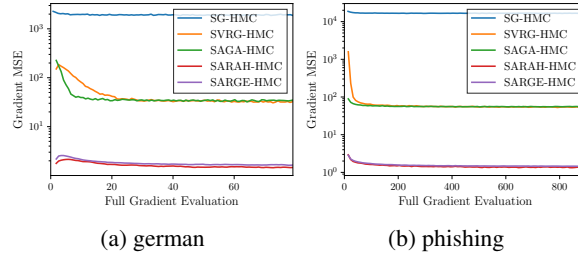


Figure 3: Gradient MSE for different algorithms.

We also report the gradient MSE of different algorithms on *german* and *phishing* datasets in Figure 3. The gradient MSE plots for the other two datasets are similar. Clearly, the biased gradient estimator (SARAH and SARGE) based methods achieve best gradient estimation. However, according to the mean potential energy and the negative log-likelihood, SARAH-HMC and SARGE-HMC are slightly worse than SVRG-HMC and SAGA-HMC. This phenomenon is once again consistent with our theoretical analysis.

5 Conclusion

We proposed a new framework of variance-reduced Hamiltonian Monte Carlo (HMC) method for sampling from an L -smooth and m -strongly log-concave distribution. The popular variance-reduction techniques, such as SAGA, SVRG, SARAH, and SARGE, can be combined with our framework. We derived the theoretical guarantee for the convergence of our framework based on the MSEB property, and we showed that all variance reduction methods considered in this paper improve the gradient complexity compared to the full gradient and stochastic gradient HMC approaches.

References

- [1] Tzuu-Shuh Chiang and Chii-Ruey Hwang. Diffusion for global optimization in rn. *SIAM J. Control Optim.*, 25(3): 737–753, May 1987.

- [2] Peter E Kloeden and Eckhard Platen. *Numerical solution of stochastic differential equations*, volume 23. Springer Science & Business Media, 2013.
- [3] Arnak S. Dalalyan. Theoretical guarantees for approximate sampling from a smooth and log-concave density. *J. R. Stat. Soc. B*, 79:651–676, 2017.
- [4] Alain Durmus and Eric Moulines. Sampling from strongly log-concave distributions with the unadjusted langevin algorithm. *arXiv preprint arXiv:1605.01559*, 5, 2016.
- [5] Arnak Dalalyan. Further and stronger analogy between sampling and optimization: Langevin monte carlo and gradient descent. In *Proceedings of the 2017 Conference on Learning Theory*, volume 65, pages 678–689, 07–10 Jul 2017.
- [6] Arnak S Dalalyan and Avetik Karagulyan. User-friendly guarantees for the langevin monte carlo with inaccurate gradient. *Stochastic Processes and their Applications*, 129(12):5278–5311, 2019.
- [7] Alain Durmus, Eric Moulines, et al. Nonasymptotic convergence analysis for the unadjusted langevin algorithm. *The Annals of Applied Probability*, 27(3):1551–1587, 2017.
- [8] Xiang Cheng and Peter Bartlett. Convergence of langevin mcmc in kl-divergence. *Proceedings of Machine Learning Research, Volume 83: Algorithmic Learning Theory*, pages 186–211, 2018.
- [9] Simon Duane, Anthony D Kennedy, Brian J Pendleton, and Duncan Roweth. Hybrid monte carlo. *Physics letters B*, 195(2):216–222, 1987.
- [10] Radford M Neal et al. Mcmc using hamiltonian dynamics. *Handbook of markov chain monte carlo*, 2(11):2, 2011.
- [11] Xiang Cheng, Niladri S. Chatterji, Peter L. Bartlett, and Michael I. Jordan. Underdamped langevin mcmc: A non-asymptotic analysis. In *Proceedings of the 31st Conference On Learning Theory*, volume 75, pages 300–323, 2018.
- [12] Yi-An Ma, Niladri Chatterji, Xiang Cheng, Nicolas Flammarion, Peter Bartlett, and Michael I Jordan. Is there an analog of nesterov acceleration for mcmc? *arXiv preprint arXiv:1902.00996*, 2019.
- [13] Max Welling and Yee Whye Teh. Bayesian learning via stochastic gradient langevin dynamics. In *Proceedings of the 28th International Conference on International Conference on Machine Learning*, page 681–688, 2011.
- [14] Yi-An Ma, Tianqi Chen, and Emily Fox. A complete recipe for stochastic gradient mcmc. In *Advances in Neural Information Processing Systems*, pages 2917–2925, 2015.
- [15] Tianqi Chen, Emily Fox, and Carlos Guestrin. Stochastic gradient hamiltonian monte carlo. In *International conference on machine learning*, pages 1683–1691, 2014.
- [16] Kumar Avinava Dubey, Sashank J Reddi, Sinead A Williamson, Barnabas Poczos, Alexander J Smola, and Eric P Xing. Variance reduction in stochastic gradient langevin dynamics. In *Advances in neural information processing systems*, pages 1154–1162, 2016.
- [17] Zhize Li, Tianyi Zhang, and Jian Li. Stochastic gradient hamiltonian monte carlo with variance reduction for bayesian inference. *Machine Learning*, 108:1701–1727, 2019.
- [18] Jack Baker, Paul Fearnhead, Emily B Fox, and Christopher Nemeth. Control variates for stochastic gradient mcmc. *Statistics and Computing*, 29(3):599–615, 2019.
- [19] Niladri S. Chatterji, Nicolas Flammarion, Yi-An Ma, Peter L. Bartlett, and Michael I. Jordan. On the theory of variance reduction for stochastic gradient monte carlo. In *ICML 2018*, volume 80, pages 763–772, 2018.
- [20] Difan Zou, Pan Xu, and Quanquan Gu. Stochastic variance-reduced hamilton monte carlo methods. In *Proceedings of the 35th International Conference on Machine Learning*, volume 80, pages 6023–6032, 2018.
- [21] Oren Mangoubi and Nisheeth Vishnoi. Dimensionally tight bounds for second-order hamiltonian monte carlo. In *Advances in neural information processing systems*, pages 6027–6037, 2018.
- [22] Yi Chen, Jinglin Chen, Jing Dong, Jian Peng, and Zhaoran Wang. Accelerating nonconvex learning via replica exchange langevin diffusion. In *7th International Conference on Learning Representations*, 2019.
- [23] Wei Deng, Qi Feng, Liyao Gao, Faming Liang, and Guang Lin. Non-convex learning via replica exchange stochastic gradient mcmc. In *Proceedings of Machine Learning and Systems 2020*, pages 2781–2790, 2020.
- [24] Aaron Defazio, Francis Bach, and Simon Lacoste-Julien. Saga: A fast incremental gradient method with support for non-strongly convex composite objectives. In *Advances in neural information processing systems*, pages 1646–1654, 2014.
- [25] Rie Johnson and Tong Zhang. Accelerating stochastic gradient descent using predictive variance reduction. In *Advances in neural information processing systems*, pages 315–323, 2013.

- [26] Lam M Nguyen, Jie Liu, Katya Scheinberg, and Martin Takáč. Sarah: A novel method for machine learning problems using stochastic recursive gradient. In *Proceedings of the 34th International Conference on Machine Learning-Volume 70*, pages 2613–2621, 2017.
- [27] Derek Driggs, Matthias J Ehrhardt, and Carola-Bibiane Schönlieb. Accelerating variance-reduced stochastic gradient methods. *arXiv preprint arXiv:1910.09494*, 2019.
- [28] Chih-Chung Chang and Chih-Jen Lin. LIBSVM: A library for support vector machines. *ACM Transactions on Intelligent Systems and Technology*, 2:27:1–27:27, 2011. Software available at <http://www.csie.ntu.edu.tw/~cjlin/libsvm>.

A Proof of Main Theory

Let Φ^t be the evolution operator of distribution regarding to the original Hamilton dynamics Eq. (5).

Let Φ_{∇}^t be the evolution operator regarding to the Hamilton dynamics conditioned on full gradient Eq. (6).

Let Φ_{∇}^t be the evolution operator regarding to the Hamilton dynamics conditioned on MSEB gradient estimator Eq. (10).

$$d\tilde{V}_t' = -\tilde{\nabla}_k dt - \gamma \xi \tilde{V}_t' dt + \sqrt{2\gamma} d\mathbf{B}_t, \quad d\tilde{X}_t' = \xi \tilde{V}_t' dt. \quad (10)$$

Let $\Phi_{\mathbb{E}\tilde{\nabla}}^t$ be the evolution operator regarding to the Hamilton dynamics conditioned on conditional expectation of MSEB gradient estimator Eq. (11).

$$d\tilde{V}_t'' = -\mathbb{E}_{k-1} \tilde{\nabla}_k dt - \gamma \xi \tilde{V}_t'' dt + \sqrt{2\gamma} d\mathbf{B}_t, \quad d\tilde{X}_t'' = \xi \tilde{V}_t'' dt. \quad (11)$$

If the initial condition $(\mathbf{x}_k, \mathbf{v}_k)$ has the distribution p_k , then the distribution of $(\mathbf{X}_t, \mathbf{V}_t)$ is $\Phi^t p_k$ and the distributions of $(\tilde{X}_t, \tilde{V}_t)$, $(\tilde{X}_t', \tilde{V}_t')$ and $(\tilde{X}_t'', \tilde{V}_t'')$ are $\Phi_{\nabla}^t p_k$, $\Phi_{\nabla}^t p_k$ and $\Phi_{\mathbb{E}\tilde{\nabla}}^t p_k$ respectively. We also denote $\Phi^t \mathbf{x}_k$ and $\Phi^t \mathbf{v}_k$ as the stochastic variable \mathbf{X}_t and \mathbf{V}_t in Eq. (5) with initial value $\mathbf{x}_k, \mathbf{v}_k$. Similarly, $\Phi_{\nabla}^t \mathbf{x}_k$ and $\Phi_{\nabla}^t \mathbf{v}_k$ represent \tilde{X}_t and \tilde{V}_t in Eq. (6) with initial value $\mathbf{x}_k, \mathbf{v}_k$.

Lemma 1. *Under same conditions of theorem 1, we have*

$$W_2^2(\Phi_{\nabla}^h q_k, \Phi^{h(k+1)} q^*) \leq A + (e^{-\frac{\delta}{4\kappa}} W_2(q_k, \Phi^{hk} q^*) + B)^2 \quad (12)$$

$$A \leq \Theta \delta^4 (4 \|\mathbf{x}_0\|_2^2 + \frac{6\kappa d}{L}) = F_1 \Theta \frac{\delta^4}{4L} \quad (13)$$

$$B \leq (1 - \rho_B) \sqrt{A} + \frac{\delta^2 (\sqrt{15\delta} + 5\sqrt{3}) \sqrt{F_2}}{60\sqrt{L}} \quad (14)$$

where $\delta = \gamma \xi h$.

Proof of lemma 1.

$$\begin{aligned} W_2^2(\Phi_{\nabla}^h q_k, \Phi^{h(k+1)} q^*) &= \mathbb{E} \left\| \Phi_{\nabla}^h q_k - \Phi_{\mathbb{E}\tilde{\nabla}}^h q_k + \Phi_{\mathbb{E}\tilde{\nabla}}^h q_k - \Phi^{h(k+1)} q^* \right\|_2^2 \\ &= \mathbb{E} \left\| \Phi_{\nabla}^h q_k - \Phi_{\mathbb{E}\tilde{\nabla}}^h q_k \right\|_2^2 + \mathbb{E} \left\| \Phi_{\mathbb{E}\tilde{\nabla}}^h q_k - \Phi^{h(k+1)} q^* \right\|_2^2 \\ &\quad + 2\mathbb{E} \langle \Phi_{\nabla}^h q_k - \Phi_{\mathbb{E}\tilde{\nabla}}^h q_k, \Phi_{\mathbb{E}\tilde{\nabla}}^h q_k - \Phi^{h(k+1)} q^* \rangle \\ &= \mathbb{E} \left\| \Phi_{\nabla}^h q_k - \Phi_{\mathbb{E}\tilde{\nabla}}^h q_k \right\|_2^2 + \mathbb{E} \left\| \Phi_{\mathbb{E}\tilde{\nabla}}^h q_k - \Phi^{h(k+1)} q^* \right\|_2^2 \\ &\quad + 2\mathbb{E}_{k-1} \langle \Phi_{\nabla}^h q_k - \Phi_{\mathbb{E}\tilde{\nabla}}^h q_k, \Phi_{\mathbb{E}\tilde{\nabla}}^h q_k - \Phi^{h(k+1)} q^* \rangle \\ &= \mathbb{E} \left\| \Phi_{\nabla}^h q_k - \Phi_{\mathbb{E}\tilde{\nabla}}^h q_k \right\|_2^2 + \mathbb{E} \left\| \Phi_{\mathbb{E}\tilde{\nabla}}^h q_k - \Phi^{h(k+1)} q^* \right\|_2^2 \end{aligned} \quad (15)$$

According to lemma 3, we can bound the first term as follows.

$$\mathbb{E} \left\| \Phi_{\nabla}^h q_k - \Phi_{\mathbb{E}\tilde{\nabla}}^h q_k \right\|_2^2 \leq \frac{\delta^2}{4L^2} \mathbb{E} \left\| \tilde{\nabla}_k - \mathbb{E} \tilde{\nabla}_k \right\|_2^2 \quad (16)$$

We further relax them term $\mathbb{E} \left\| \tilde{\nabla}_k - \mathbb{E} \tilde{\nabla}_k \right\|_2^2$ into $\mathbb{E} \left\| \tilde{\nabla}_k - \nabla f(\mathbf{x}_k) \right\|_2^2$ whose upper bound can be found at lemma 7.

We split the second term further.

$$\begin{aligned}
\mathbb{E} \left\| \Phi_{\mathbb{E} \tilde{\nabla}}^h q_k - \Phi^{h(k+1)} q^* \right\|_2^2 &= \mathbb{E} \left\| \Phi_{\mathbb{E} \tilde{\nabla}}^h q_k - \Phi_{\nabla}^h q_k \right. \\
&\quad \left. + \Phi_{\nabla}^h q_k - \Phi^{h(k+1)} q^* \right\|_2^2 \\
&\leq \left(\sqrt{\mathbb{E} \left\| \Phi_{\mathbb{E} \tilde{\nabla}}^h q_k - \Phi_{\nabla}^h q_k \right\|_2^2} \right. \\
&\quad \left. + \sqrt{\mathbb{E} \left\| \Phi_{\nabla}^h q_k - \Phi^{h(k+1)} q^* \right\|_2^2} \right)^2
\end{aligned} \tag{17}$$

The first term in the last line of Eq. (17) is controlled in lemma 4.

We split the second term in the last line of Eq. (17) as follows.

$$\sqrt{\mathbb{E} \left\| \Phi_{\nabla}^h q_k - \Phi^h q_k \right\|_2^2} \leq 2 \sqrt{\mathbb{E} \left\| \Phi_{\nabla}^h x_k - \Phi^h x_k \right\|_2^2} + \sqrt{\mathbb{E} \left\| \Phi_{\nabla}^h v_k - \Phi^h v_k \right\|_2^2} \tag{18}$$

In lemma 5, we show that both these two terms can be controlled by momentum $\max_{r < h} \mathbb{E} \left\| \mathbf{V}_r \right\|_2^2 = \max_{r < h} \mathbb{E} \left\| \Phi^h \mathbf{v}_k \right\|_2^2$ as follows.

$$\begin{aligned}
\sqrt{\mathbb{E} \left\| \Phi_{\nabla}^h q_k - \Phi^h q_k \right\|_2^2} &\leq 2 \sqrt{\mathbb{E} \left\| \Phi_{\nabla}^h x_k - \Phi^h x_k \right\|_2^2} + \sqrt{\mathbb{E} \left\| \Phi_{\nabla}^h v_k - \Phi^h v_k \right\|_2^2} \\
&\leq \frac{2}{\sqrt{15}} h^3 L^3 \sqrt{\mathbb{E} \left\| \Phi_{\nabla}^h v_k \right\|_2^2} + \frac{1}{\sqrt{3}} h^2 L^2 \sqrt{\mathbb{E} \left\| \Phi_{\nabla}^h v_k \right\|_2^2}
\end{aligned} \tag{19}$$

By assuming small step size, we can also derive an upper bound for the momentum in lemma 6.

The third term in the last line of Eq. (17) decreases due to the contraction property of HMC on a strongly log-concave distribution. According to [11, Theorem 5], the following inequality holds.

$$\begin{aligned}
\mathbb{E} \left\| \Phi^h q_k - \Phi^{h(k+1)} q^* \right\|_2^2 &\leq W_2^2(\Phi^h q_k, \Phi^{h(k+1)} q^*) \\
&\leq e^{-\frac{\delta}{2\kappa}} W_2^2(q_k, \Phi^{hk} q^*)
\end{aligned} \tag{20}$$

Combining all above upper bounds for each term give rise to the final upper bound. \square

Proof of theorem 1. By Lemma 7 of [6], if $x_{k+1}^2 \leq ((1 - \alpha)x_k + B)^2 + A$, then

$$x_k \leq (1 - \alpha)^k x_0 + \frac{B}{\alpha} + \frac{A}{B + \sqrt{\alpha(2 - \alpha)A}} \leq (1 - \alpha)^k x_0 + \frac{B}{\alpha} + \frac{\sqrt{A}}{\sqrt{\alpha}} \tag{21}$$

Because our step size is small enough, we have

$$e^{-\frac{\delta}{4\kappa}} < 1 - \frac{\delta}{8\kappa}$$

We apply inequality Eq. (21) into lemma 1 to finish the proof.

$$\begin{aligned}
W_2(\Phi_{\nabla}^h q_k, \Phi^{h(k+1)} q^*) &\leq e^{-\frac{k\delta}{4\kappa}} W_2(q_0, q^*) + \frac{8\kappa}{\delta} B + \frac{\sqrt{8\kappa}}{\sqrt{\delta}} \sqrt{A} \\
&\leq e^{-\frac{k\delta}{4\kappa}} W_2(q_0, q^*) + 8\sqrt{LF_2\kappa}h \\
&\quad + 4\sqrt{\Theta F_1} \left(2(1 - \rho_B) \sqrt{L\kappa}h + L\sqrt{\kappa}h^{\frac{3}{2}} \right)
\end{aligned} \tag{22}$$

\square

B Technical Lemmas

Lemma 2. In Eq. (6), if we choose two different gradient $\tilde{\nabla}_k$ and ∇_k to generate two different SDE with same initial distribution q_k , the Wasserstein distance of distribution of $\Phi_{\tilde{\nabla}}^h q_k$ and $\Phi_{\nabla}^h q_k$ can be upper bounded by the gradient difference in the following way.

$$\mathbb{E} \left\| \Phi_{\tilde{\nabla}}^h q_k - \Phi_{\nabla}^h q_k \right\|_2^2 \leq \frac{\delta^2}{4L^2} \mathbb{E} \left\| \tilde{\nabla}_k - \nabla_k \right\|_2^2 \quad (23)$$

The above inequality holds true for all positive step size.

Proof of lemma 2.

$$\begin{aligned} \mathbb{E} \left\| \Phi_{\tilde{\nabla}}^h q_k - \Phi_{\nabla}^h q_k \right\|_2^2 &= \mathbb{E} \left\| \Phi_{\tilde{\nabla}}^h \mathbf{x}_k - \Phi_{\nabla}^h \mathbf{x}_k \right\|_2^2 \\ &\quad + \mathbb{E} \left\| \Phi_{\tilde{\nabla}}^h \mathbf{x}_k - \Phi_{\nabla}^h \mathbf{x}_k + \Phi_{\tilde{\nabla}}^h \mathbf{v}_k - \Phi_{\nabla}^h \mathbf{v}_k \right\|_2^2 \\ &= \left(\frac{\nabla_k \left(h - \frac{1-e^{-\gamma h \xi}}{\gamma \xi} \right)}{\gamma} - \frac{\tilde{\nabla}_k \left(h - \frac{1-e^{-\gamma h \xi}}{\gamma \xi} \right)}{\gamma} \right)^2 \\ &\quad + \left(\frac{\nabla_k \left(h - \frac{1-e^{-\gamma h \xi}}{\gamma \xi} \right)}{\gamma} + \frac{\nabla_k (1 - e^{-\gamma h \xi})}{\gamma \xi} \right. \\ &\quad \left. - \frac{\tilde{\nabla}_k \left(h - \frac{1-e^{-\gamma h \xi}}{\gamma \xi} \right)}{\gamma} - \frac{\tilde{\nabla}_k (1 - e^{-\gamma h \xi})}{\gamma \xi} \right)^2 \\ &= \frac{(\tilde{\nabla}_k - \nabla_k)^2 e^{-2\gamma h \xi}}{\gamma^4 \xi^2} \times \left((\gamma h \xi e^{\gamma h \xi} - e^{\gamma h \xi} + 1)^2 \right. \\ &\quad \left. + (-\gamma h \xi e^{\gamma h \xi} + \gamma (1 - e^{\gamma h \xi}) + e^{\gamma h \xi} - 1)^2 \right) \\ &= \frac{(\tilde{\nabla}_k - \nabla_k)^2 ((\delta^2 + 1) e^{2\delta} - 2e^\delta + 1) e^{-2\delta}}{8L^2} \\ &\leq \frac{(\tilde{\nabla}_k - \nabla_k)^2 \delta^2}{4L^2} \end{aligned} \quad (24)$$

The last inequality doesn't depend on any assumption of small step size. \square

Lemma 3.

$$\begin{aligned} \mathbb{E} \left\| \Phi_{\tilde{\nabla}}^h q_k - \Phi_{\mathbb{E}\tilde{\nabla}}^h q_k \right\|_2^2 &= \mathbb{E} \left\| (d\tilde{\mathbf{X}}'_h - d\tilde{\mathbf{X}}''_h, d\tilde{\mathbf{X}}'_h - d\tilde{\mathbf{X}}''_h + d\tilde{\mathbf{V}}'_h - d\tilde{\mathbf{V}}''_h) \right\|_2^2 \\ &\leq \frac{\delta^2}{4L^2} \mathbb{E} \left\| \tilde{\nabla}_k - \mathbb{E}\tilde{\nabla}_k \right\|_2^2 \end{aligned} \quad (25)$$

Proof of lemma 3. This is just a special case of lemma 2. \square

Lemma 4.

$$\mathbb{E} \left\| \Phi_{\mathbb{E}\tilde{\nabla}}^h q_k - \Phi_{\nabla}^h q_k \right\|_2^2 \leq \frac{\delta^2}{4L^2} \mathbb{E} \left\| \mathbb{E}_{k-1} \tilde{\nabla}_k - \nabla f(\mathbf{x}_k) \right\|_2^2 \quad (26)$$

$$\leq \frac{\delta^2}{4L^2} (1 - \rho_B)^2 \mathbb{E} \left\| \tilde{\nabla}_{k-1} - \nabla f(\mathbf{x}_{k-1}) \right\|_2^2 \quad (27)$$

Proof of lemma 4. The first inequality comes from lemma 2, and the second inequality comes from MSEB property. \square

Lemma 5.

$$\mathbb{E} \left\| \Phi_{\tilde{\nabla}}^h \mathbf{v}_k - \Phi^h \mathbf{v}_k \right\|_2^2 \leq \frac{1}{3} h^4 L^4 \max_{r < h} \mathbb{E} \left\| \mathbf{V}_r \right\|_2^2 \quad (28)$$

$$\mathbb{E} \|\Phi_{\nabla}^h \mathbf{x}_k - \Phi^h \mathbf{x}_k\|_2^2 \leq \frac{1}{15} h^6 L^6 \max_{r < h} \mathbb{E} \|\mathbf{V}_r\|_2^2 \quad (29)$$

Proof of lemma 5.

$$\begin{aligned} \mathbb{E} \|\Phi_{\nabla}^h \mathbf{v}_k - \Phi^h \mathbf{v}_k\|_2^2 &\leq \mathbb{E} \left\| \int_0^h e^{-\gamma \xi(h-s)} (\nabla f(\mathbf{X}_s) - \nabla f(\mathbf{x}_k)) ds \right\|_2^2 \\ &\leq h \int_0^h \mathbb{E} \left\| e^{-\gamma \xi(h-s)} (\nabla f(\mathbf{X}_s) - \nabla f(\mathbf{x}_k)) \right\|_2^2 ds \\ &\leq h L^2 \int_0^h \mathbb{E} \|\mathbf{X}_s - \mathbf{x}_k\|_2^2 ds \\ &\leq h L^2 \int_0^h \mathbb{E} \left\| \int_0^s \xi \mathbf{V}_r dr \right\|_2^2 ds \\ &\leq h L^2 \xi^2 \int_0^h s \int_0^s \mathbb{E} \|\mathbf{V}_r\|_2^2 dr ds \\ &\leq \frac{1}{3} h^4 L^4 \max_{r < h} \mathbb{E} \|\mathbf{V}_r\|_2^2 \end{aligned} \quad (30)$$

$$\begin{aligned} \mathbb{E} \|\Phi_{\nabla}^h \mathbf{x}_k - \Phi^h \mathbf{x}_k\|_2^2 &= \mathbb{E} \left\| \int_0^h \xi (\Phi_{\nabla}^s \mathbf{v}_k - \Phi^s \mathbf{v}_k) ds \right\|_2^2 \\ &\leq h \xi^2 \int_0^h \mathbb{E} \|\Phi_{\nabla}^s \mathbf{v}_k - \Phi^s \mathbf{v}_k\|_2^2 ds \\ &\leq \frac{1}{15} h^6 L^6 \max_{r < h} \mathbb{E} \|\mathbf{V}_r\|_2^2 \end{aligned} \quad (31)$$

□

Lemma 6. *With small step size assumption, we have the momentum bounded as follows.*

$$\mathbb{E} \|\Phi^h \mathbf{v}_k\|_2^2 \leq 97 \|\mathbf{x}_0\|_2^2 + \frac{181 \kappa d}{L} \quad (32)$$

Proof of lemma 6. We control the momentum in a recursive way.

First we show that $\mathbb{E} \|\mathbf{V}_h\|_2^2$ and $\mathbb{E} \|\mathbf{X}_h\|_2^2$ can be controlled by step change $\mathbb{E} \|\Phi^h \mathbf{v}_k - \mathbf{v}_k\|_2^2$ and $\mathbb{E} \|\Phi^h \mathbf{x}_k - \mathbf{x}_k\|_2^2$, and then we show that the reverse is also true.

$$\begin{aligned} \mathbb{E} \|\mathbf{V}_h\|_2^2 &= \mathbb{E} \|\Phi^h \mathbf{v}_k\|_2^2 \\ &\leq 2 \mathbb{E} \|\Phi^h \mathbf{v}_k - \mathbf{v}_k\|_2^2 + 2 \mathbb{E} \|\mathbf{v}_k\|_2^2 \end{aligned} \quad (33)$$

$$\begin{aligned} \mathbb{E} \|\mathbf{X}_h\|_2^2 &= \mathbb{E} \|\Phi^h \mathbf{x}_k\|_2^2 \\ &\leq 2 \mathbb{E} \|\Phi^h \mathbf{x}_k - \mathbf{x}_k\|_2^2 + 2 \mathbb{E} \|\mathbf{x}_k\|_2^2 \end{aligned} \quad (34)$$

$$\begin{aligned} \mathbb{E} \|\Phi^h \mathbf{v}_k - \mathbf{v}_k\|_2^2 &= \mathbb{E} \left\| \int_0^h e^{-\gamma \xi(h-s)} \nabla f(\mathbf{X}_s) ds \right\|_2^2 + 2\gamma \mathbb{E} \left\| \int_0^h e^{-\gamma \xi(h-s)} d\mathbf{B}_s \right\|_2^2 \\ &\leq h \int_0^h \mathbb{E} \|\nabla f(\mathbf{X}_s)\|_2^2 ds + \frac{1}{\xi} (1 - e^{-\gamma \xi h}) \\ &\leq h L^2 \int_0^h \mathbb{E} \|\mathbf{X}_s\|_2^2 ds + \frac{1}{\xi} (1 - e^{-\gamma \xi h}) \\ &\leq h^2 L^2 \max_{r < h} \mathbb{E} \|\mathbf{X}_r\|_2^2 ds + \gamma h \end{aligned} \quad (35)$$

$$\begin{aligned}
\mathbb{E} \|\Phi^h \mathbf{x}_k - \mathbf{x}_k\|_2^2 &= \mathbb{E} \left\| \int_0^h \xi \mathbf{V}_s ds \right\|_2^2 \\
&\leq h \xi^2 \int_0^h \mathbb{E} \|\mathbf{V}_s\|_2^2 ds \\
&\leq h^2 L^2 \max_{r < h} \mathbb{E} \|\mathbf{V}_r\|_2^2 ds
\end{aligned} \tag{36}$$

Combine the above four equation, we can see that

$$\begin{aligned}
\mathbb{E} \|\Phi^h \mathbf{v}_k\|_2^2 &\leq 2h^2 L^2 \max_{r < h} \mathbb{E} \|\Phi^r \mathbf{x}_k\|_2^2 + 2\gamma h + 2\mathbb{E} \|\mathbf{v}_k\|_2^2 \\
\mathbb{E} \|\Phi^h \mathbf{x}_k\|_2^2 &\leq 2h^2 L^2 \max_{r < h} \mathbb{E} \|\Phi^r \mathbf{v}_k\|_2^2 + 2\mathbb{E} \|\mathbf{x}_k\|_2^2
\end{aligned} \tag{37}$$

This further imply following inequality.

$$\mathbb{E} \|\Phi^h \mathbf{v}_k\|_2^2 \leq 4h^4 L^4 \max_{r < h} \mathbb{E} \|\Phi^r \mathbf{v}_k\|_2^2 + 4h^2 L^2 \mathbb{E} \|\mathbf{x}_k\|_2^2 + 2\gamma h + 2\mathbb{E} \|\mathbf{v}_k\|_2^2 \tag{38}$$

We finish the proof by applying Gronwall's inequality and substitute $\mathbb{E} \|\mathbf{v}_k\|_2^2$ and $\mathbb{E} \|\mathbf{x}_k\|_2^2$ with their upper bound in lemma 7. \square

Lemma 7. *With small enough step size δ satisfying $\delta \leq \frac{1}{5\kappa} \min(1, \frac{1}{\sqrt{\Theta}})$, the following inequalities holds.*

$$\begin{aligned}
\max_k \mathbb{E} (E(\mathbf{x}_k, \mathbf{v}_k)) &\leq 24 \|\mathbf{x}_0\|_2^2 + \frac{45\kappa d}{L} \\
\max_k \mathbb{E} \|\mathbf{x}_k\|_2^2 &\leq 24 \|\mathbf{x}_0\|_2^2 + \frac{45\kappa d}{L} \\
\max_k \mathbb{E} \|\mathbf{v}_k\|_2^2 &\leq 48 \|\mathbf{x}_0\|_2^2 + \frac{89\kappa d}{L} \\
\max_k \mathbb{E} \|\nabla f(\mathbf{x}_k)\|_2^2 &\leq 24L^2 \|\mathbf{x}_0\|_2^2 + 45L\kappa d \\
\max_k \mathbb{E} \|\tilde{\nabla}_k - \nabla f(\mathbf{x}_k)\|_2^2 &\leq 13L^2 \Theta \delta^2 \|\mathbf{x}_0\|_2^2 + 24L\Theta \delta^2 \kappa d \\
\max_k Q_k &\leq 13L^2 \delta^2 \|\mathbf{x}_0\|_2^2 + 24L\delta^2 \kappa d
\end{aligned} \tag{39}$$

where $E(\mathbf{x}, \mathbf{v}) = \|\mathbf{x}\|_2^2 + \left\| \mathbf{x} + \frac{2}{\gamma} \mathbf{v} \right\|_2^2 + \frac{8}{\xi \gamma^2} (f(\mathbf{x}) - f(\mathbf{x}^*))$ is the Lyapunov function.

Proof of lemma 7. lemmas 8 to 11 show preliminary results of upper bounds.

We further control coefficients in lemmas 8 and 11. If we have $\delta \leq \frac{17}{32}$, we can relax the coefficients of eqs. (45) and (54) into

$$\begin{aligned}
\max_k \mathbb{E} (E(\mathbf{x}_k, \mathbf{v}_k)) &\leq \frac{5\delta\kappa \max_k \mathbb{E} \|\mathbf{x}_k\|_2^2}{2} + \max_k \mathbb{E} \|\tilde{\nabla}_k - \nabla f(\mathbf{x}_k)\|_2^2 u_{135} \\
&\quad + 6 \|\mathbf{x}_0\|_2^2 + du_{138}
\end{aligned} \tag{40}$$

$$\begin{aligned}
\max_k Q_k &\leq \frac{L^2 \delta^3 \max_k \mathbb{E} \|\mathbf{x}_k\|_2^2}{8} + \frac{L^2 \delta^2 \max_k \mathbb{E} \|\mathbf{v}_k\|_2^2}{4} + \frac{L\delta^3 d}{6} \\
&\quad + \frac{5\delta^3 \max_k \mathbb{E} \|\tilde{\nabla}_k - \nabla f(\mathbf{x}_k)\|_2^2}{64}
\end{aligned} \tag{41}$$

Variables u_i are used to simplify the formula. The definition of u_i can be found at the end of this section.

By applying eqs. (47) and (48) into Eq. (40), we can show that

$$\max_k \mathbb{E} (E(\mathbf{x}_k, \mathbf{v}_k)) \leq \max_k \mathbb{E} \left\| \tilde{\nabla}_k - \nabla f(\mathbf{x}_k) \right\|_2^2 u_{146} + 12 \|\mathbf{x}_0\|_2^2 + du_{147} \quad (42)$$

whenever $\frac{5\delta\kappa}{2} \leq \frac{1}{2}$.

By applying eqs. (42), (47), (48) and (50) into Eq. (50), we can show that

$$\max_k \mathbb{E} \left\| \tilde{\nabla}_k - \nabla f(\mathbf{x}_k) \right\|_2^2 \leq \|\mathbf{x}_0\|_2^2 u_{161} + du_{160} \quad (43)$$

whenever $\frac{5\Theta\delta^3\kappa^2}{4} + \frac{25\Theta\delta^3\kappa}{16} + \frac{5\Theta\delta^3}{64} + 5\Theta\delta^2\kappa^2 + \frac{25\Theta\delta^2\kappa}{4} \leq \frac{1}{2}$.

Applying Eq. (43) back into Eq. (42) gives

$$\max_k \mathbb{E} (E(\mathbf{x}_k, \mathbf{v}_k)) \leq \|\mathbf{x}_0\|_2^2 u_{159} + du_{158} \quad (44)$$

We then apply eqs. (43) and (44) into eqs. (41) and (47) to (49) and relax δ into lowest order and relax κ into highest order to generate the final result. \square

Lemma 8.

$$\begin{aligned} \max_k \mathbb{E} (E(\mathbf{x}_k, \mathbf{v}_k)) &\leq \max_k \mathbb{E} \|\mathbf{v}_k\|_2^2 u_{101} + \max_k \mathbb{E} \|\mathbf{x}_k\|_2^2 u_{102} \\ &\quad + \max_k \mathbb{E} \left\| \tilde{\nabla}_k - \nabla f(\mathbf{x}_k) \right\|_2^2 u_{100} + 6 \|\mathbf{x}_0\|_2^2 + du_{104} \end{aligned} \quad (45)$$

where expressions u_i can be found at the end of this section.

Proof of lemma 8.

$$\begin{aligned}
& \mathbb{E}E(\mathbf{x}_{k+1}, \mathbf{v}_{k+1}) - \mathbb{E}(E(\mathbf{x}_k, \mathbf{v}_k)) \left(1 - \frac{\delta}{10\kappa}\right) \\
&= \mathbb{E}\langle \mathbf{v}_k, \mathbf{x}_k \rangle u_{27} + 2\mathbb{E}\langle \mathbf{v}_{k+1}, \mathbf{x}_{k+1} \rangle + \mathbb{E}\|\mathbf{v}_k\|_2^2 u_{18} + \mathbb{E}\|\mathbf{v}_{k+1}\|_2^2 + \mathbb{E}\|\mathbf{x}_k\|_2^2 u_{27} \\
&\quad + 2\mathbb{E}\|\mathbf{x}_{k+1}\|_2^2 + f(\mathbf{x}_k)u_{24} - \frac{\delta f(\mathbf{x}^*)}{5L\kappa} + \frac{2f(\mathbf{x}_{k+1})}{L} \\
&\leq -\frac{\delta \mathbb{E}\langle \mathbf{x}^*, \mathbf{x}_k \rangle}{5\kappa} + \frac{\delta \|\mathbf{x}^*\|_2^2}{10\kappa} + \mathbb{E}\langle \mathbf{v}_k, \mathbf{x}_k \rangle u_{27} + 2\mathbb{E}\langle \mathbf{v}_{k+1}, \mathbf{x}_{k+1} \rangle - 2\mathbb{E}\langle \mathbf{x}_{k+1}, \mathbf{x}_k \rangle \\
&\quad + \mathbb{E}\|\mathbf{v}_k\|_2^2 u_{18} + \mathbb{E}\|\mathbf{v}_{k+1}\|_2^2 + \mathbb{E}\|\mathbf{x}_k\|_2^2 u_{32} + 3\mathbb{E}\|\mathbf{x}_{k+1}\|_2^2 - \frac{2\mathbb{E}\langle \nabla f(\mathbf{x}_k), \mathbf{x}_k \rangle}{L} \\
&\quad + \frac{2\mathbb{E}\langle \nabla f(\mathbf{x}_k), \mathbf{x}_{k+1} \rangle}{L} \\
&= \mathbb{E}\langle \mathbf{v}_k, \mathbf{x}_k \rangle u_{27} + 2\mathbb{E}\langle \mathbf{v}_{k+1}, \mathbf{x}_{k+1} \rangle - 2\mathbb{E}\langle \mathbf{x}_{k+1}, \mathbf{x}_k \rangle + \mathbb{E}\|\mathbf{v}_k\|_2^2 u_{18} + \mathbb{E}\|\mathbf{v}_{k+1}\|_2^2 \\
&\quad + \mathbb{E}\|\mathbf{x}_k\|_2^2 u_{32} + 3\mathbb{E}\|\mathbf{x}_{k+1}\|_2^2 - \frac{2\mathbb{E}\langle \nabla f(\mathbf{x}_k), \mathbf{x}_k \rangle}{L} + \frac{2\mathbb{E}\langle \nabla f(\mathbf{x}_k), \mathbf{x}_{k+1} \rangle}{L} \\
&= \frac{\delta \mathbb{E}\langle \mathbf{v}_k, \mathbf{x}_k \rangle}{5\kappa} + \frac{3\delta \mathbb{E}\|\mathbf{x}_k\|_2^2}{10\kappa} + 2\mathbb{E}\langle \mathbf{e}_k^v, \mathbf{e}_k^x \rangle + \mathbb{E}\langle \mathbf{e}_k^v, \mathbf{v}_k \rangle u_{62} + 2\mathbb{E}\langle \mathbf{e}_k^v, \mathbf{x}_k \rangle \\
&\quad + \mathbb{E}\langle \mathbf{e}_k^x, \mathbf{v}_k \rangle u_{61} + 4\mathbb{E}\langle \mathbf{e}_k^x, \mathbf{x}_k \rangle + \mathbb{E}\langle \nabla f(\mathbf{x}_k), \mathbf{v}_k \rangle u_{63} + \mathbb{E}\langle \tilde{\nabla}_k, \mathbf{e}_k^v \rangle u_{53} \\
&\quad + \mathbb{E}\langle \tilde{\nabla}_k, \mathbf{e}_k^x \rangle u_{52} + \mathbb{E}\langle \tilde{\nabla}_k, \mathbf{v}_k \rangle u_{60} + \mathbb{E}\langle \tilde{\nabla}_k, \nabla f(\mathbf{x}_k) \rangle u_{56} + \mathbb{E}\|\mathbf{e}_k^v\|_2^2 + 3\mathbb{E}\|\mathbf{e}_k^x\|_2^2 \\
&\quad + \mathbb{E}\|\mathbf{v}_k\|_2^2 u_{64} + \mathbb{E}\|\tilde{\nabla}_k\|_2^2 u_{47} - \frac{\delta \mathbb{E}\langle \tilde{\nabla}_k, \mathbf{x}_k \rangle}{L} + \frac{2\mathbb{E}\langle \nabla f(\mathbf{x}_k), \mathbf{e}_k^x \rangle}{L} \\
&= \frac{\delta \mathbb{E}\langle \mathbf{v}_k, \mathbf{x}_k \rangle}{5\kappa} + \frac{3\delta \mathbb{E}\|\mathbf{x}_k\|_2^2}{10\kappa} + \mathbb{E}\langle \nabla f(\mathbf{x}_k), \mathbf{v}_k \rangle u_{73} + \mathbb{E}\langle \tilde{\nabla}_k - \nabla f(\mathbf{x}_k), \mathbf{v}_k \rangle u_{60} \\
&\quad + \mathbb{E}\langle \tilde{\nabla}_k - \nabla f(\mathbf{x}_k), \nabla f(\mathbf{x}_k) \rangle u_{70} + \mathbb{E}\|\mathbf{v}_k\|_2^2 u_{64} + \mathbb{E}\|\nabla f(\mathbf{x}_k)\|_2^2 u_{72} \\
&\quad + \mathbb{E}\|\tilde{\nabla}_k - \nabla f(\mathbf{x}_k)\|_2^2 u_{47} + du_{68} - \frac{\delta \mathbb{E}\langle \nabla f(\mathbf{x}_k), \mathbf{x}_k \rangle}{L} - \frac{\delta \mathbb{E}\langle \tilde{\nabla}_k - \nabla f(\mathbf{x}_k), \mathbf{x}_k \rangle}{L} \\
&\leq \frac{\delta \mathbb{E}\langle \mathbf{v}_k, \mathbf{x}_k \rangle}{5\kappa} - \frac{7\delta \mathbb{E}\|\mathbf{x}_k\|_2^2}{10\kappa} + \mathbb{E}\langle \nabla f(\mathbf{x}_k), \mathbf{v}_k \rangle u_{73} + \mathbb{E}\langle \tilde{\nabla}_k - \nabla f(\mathbf{x}_k), \mathbf{v}_k \rangle u_{60} \\
&\quad + \mathbb{E}\langle \tilde{\nabla}_k - \nabla f(\mathbf{x}_k), \nabla f(\mathbf{x}_k) \rangle u_{70} + \mathbb{E}\|\mathbf{v}_k\|_2^2 u_{64} + \mathbb{E}\|\nabla f(\mathbf{x}_k)\|_2^2 u_{72} \\
&\quad + \mathbb{E}\|\tilde{\nabla}_k - \nabla f(\mathbf{x}_k)\|_2^2 u_{47} + du_{68} - \frac{\delta \mathbb{E}\langle \tilde{\nabla}_k - \nabla f(\mathbf{x}_k), \mathbf{x}_k \rangle}{L} \\
&\leq \frac{\delta \mathbb{E}\langle \mathbf{v}_k, \mathbf{x}_k \rangle}{5\kappa} - \frac{7\delta \mathbb{E}\|\mathbf{x}_k\|_2^2}{10\kappa} + \mathbb{E}\langle \tilde{\nabla}_k - \nabla f(\mathbf{x}_k), \mathbf{v}_k \rangle u_{60} + \mathbb{E}\|\mathbf{v}_k\|_2^2 u_{87} \\
&\quad + \mathbb{E}\|\nabla f(\mathbf{x}_k)\|_2^2 u_{86} + \mathbb{E}\|\tilde{\nabla}_k - \nabla f(\mathbf{x}_k)\|_2^2 u_{80} + du_{68} - \frac{\delta \mathbb{E}\langle \tilde{\nabla}_k - \nabla f(\mathbf{x}_k), \mathbf{x}_k \rangle}{L} \\
&\leq \frac{\delta \mathbb{E}\langle \mathbf{v}_k, \mathbf{x}_k \rangle}{5\kappa} + \mathbb{E}\langle \tilde{\nabla}_k - \nabla f(\mathbf{x}_k), \mathbf{v}_k \rangle u_{60} + \mathbb{E}\|\mathbf{v}_k\|_2^2 u_{87} + \mathbb{E}\|\mathbf{x}_k\|_2^2 u_{89} \\
&\quad + \mathbb{E}\|\tilde{\nabla}_k - \nabla f(\mathbf{x}_k)\|_2^2 u_{80} + du_{68} - \frac{\delta \mathbb{E}\langle \tilde{\nabla}_k - \nabla f(\mathbf{x}_k), \mathbf{x}_k \rangle}{L} \\
&\leq \mathbb{E}\|\mathbf{v}_k\|_2^2 u_{96} + \mathbb{E}\|\mathbf{x}_k\|_2^2 u_{88} + \mathbb{E}\|\tilde{\nabla}_k - \nabla f(\mathbf{x}_k)\|_2^2 u_{93} + du_{68} \\
&\leq \mathbb{E}\|\mathbf{v}_k\|_2^2 \max(0, u_{96}) + \mathbb{E}\|\mathbf{x}_k\|_2^2 u_{88} + \mathbb{E}\|\tilde{\nabla}_k - \nabla f(\mathbf{x}_k)\|_2^2 \max(0, u_{93}) + du_{68}
\end{aligned} \tag{46}$$

The first inequality comes from Lipschitz condition.

The second inequality comes from strongly convex condition of $f(\mathbf{x})$.

The third inequality comes from Young's inequalities.

$$\begin{aligned}\mathbb{E}\langle \nabla f(\mathbf{x}_k), \mathbf{v}_k \rangle &\leq \frac{L\mathbb{E}\|\mathbf{v}_k\|_2^2}{4} + \frac{\mathbb{E}\|\nabla f(\mathbf{x}_k)\|_2^2}{L} \\ \mathbb{E}\langle \tilde{\nabla}_k - \nabla f(\mathbf{x}_k), \nabla f(\mathbf{x}_k) \rangle &\leq \frac{\delta\mathbb{E}\|\nabla f(\mathbf{x}_k)\|_2^2}{2} + \frac{\mathbb{E}\|\tilde{\nabla}_k - \nabla f(\mathbf{x}_k)\|_2^2}{2\delta}\end{aligned}$$

The fourth inequality comes from Lipschitz condition.

The fifth inequality comes from Young's inequalities.

$$\begin{aligned}\mathbb{E}\langle \mathbf{v}_k, \mathbf{x}_k \rangle &\leq \frac{\mathbb{E}\|\mathbf{v}_k\|_2^2}{4} + \mathbb{E}\|\mathbf{x}_k\|_2^2 \\ \mathbb{E}\langle \tilde{\nabla}_k - \nabla f(\mathbf{x}_k), \mathbf{x}_k \rangle &\leq \frac{L\mathbb{E}\|\mathbf{x}_k\|_2^2}{2\kappa} + \frac{\kappa\mathbb{E}\|\tilde{\nabla}_k - \nabla f(\mathbf{x}_k)\|_2^2}{2L} \\ \mathbb{E}\langle \tilde{\nabla}_k - \nabla f(\mathbf{x}_k), \mathbf{v}_k \rangle &\leq \frac{L\mathbb{E}\|\mathbf{v}_k\|_2^2}{2} + \frac{\mathbb{E}\|\tilde{\nabla}_k - \nabla f(\mathbf{x}_k)\|_2^2}{2L}\end{aligned}$$

We apply Gronwall's inequality on Eq. (46) to finish the proof. \square

Lemma 9.

$$\max_k \mathbb{E}\|\mathbf{x}_k\|_2^2 \leq \max_k \mathbb{E}(E(\mathbf{x}_k, \mathbf{v}_k)) \quad (47)$$

$$\max_k \mathbb{E}\|\mathbf{v}_k\|_2^2 \leq 2 \max_k \mathbb{E}(E(\mathbf{x}_k, \mathbf{v}_k)) \quad (48)$$

$$\max_k \mathbb{E}\|\nabla f(\mathbf{x}_k)\|_2^2 \leq L^2 \max_k \mathbb{E}\|\mathbf{x}_k\|_2^2 \quad (49)$$

Proof of lemma 9. These inequalities follows from definition of E and Lipschitz condition. \square

Lemma 10.

$$\max_k \mathbb{E}\|\tilde{\nabla}_k - \nabla f(\mathbf{x}_k)\|_2^2 \leq \Theta \max_k Q_k \quad (50)$$

where $\Theta = \frac{M_1}{\rho_M} + \frac{M_2}{\rho_M \rho_F}$.

Proof of lemma 10.

$$\begin{aligned}\mathcal{M}_k &\leq M_1 Q_k + \mathcal{F}_k + (1 - \rho_M) \mathcal{M}_{k-1} \\ &\leq M_1 \sum_{i=0}^k (1 - \rho_M)^i Q_{k-i} + \sum_{i=0}^k (1 - \rho_M)^{k-i} \mathcal{F}_i\end{aligned} \quad (51)$$

$$M_1 \sum_{i=0}^k (1 - \rho_M)^i Q_{k-i} \leq \frac{M_1}{\rho_M} \max_k Q_k \quad (52)$$

$$\begin{aligned}\sum_{i=0}^k (1 - \rho_M)^{k-i} \mathcal{F}_i &\leq M_2 \sum_{i=0}^k \sum_{l=0}^i (1 - \rho_F)^{i-l} (1 - \rho_M)^{k-i} Q_l \\ &\leq \frac{M_2}{\rho_M \rho_F} \max_k Q_k\end{aligned} \quad (53)$$

\square

Lemma 11.

$$\begin{aligned}\max_k Q_k &\leq \max_k \mathbb{E}\|\mathbf{v}_k\|_2^2 u_{127} + \max_k \mathbb{E}\|\mathbf{x}_k\|_2^2 u_{124} \\ &\quad + \max_k \mathbb{E}\|\tilde{\nabla}_k - \nabla f(\mathbf{x}_k)\|_2^2 u_{126} + du_{105}\end{aligned} \quad (54)$$

Proof of lemma 11.

$$\begin{aligned}
Q_k &= N \sum_{i=1}^N \mathbb{E} \|\nabla f_i(\mathbf{x}_{k+1}) - \nabla f_i(\mathbf{x}_k)\|_2^2 \\
&\leq -2L^2 \mathbb{E} \langle \mathbf{x}_{k+1}, \mathbf{x}_k \rangle + L^2 \mathbb{E} \|\mathbf{x}_k\|_2^2 + L^2 \mathbb{E} \|\mathbf{x}_{k+1}\|_2^2 \\
&= \mathbb{E} \langle \tilde{\nabla}_k, \mathbf{v}_k \rangle u_{111} + \mathbb{E} \|\mathbf{v}_k\|_2^2 u_{113} + \mathbb{E} \|\tilde{\nabla}_k\|_2^2 u_{109} + du_{105} \\
&= \mathbb{E} \langle \nabla f(\mathbf{x}_k), \mathbf{v}_k \rangle u_{111} + \mathbb{E} \langle \tilde{\nabla}_k - \nabla f(\mathbf{x}_k), \mathbf{v}_k \rangle u_{111} \\
&\quad + \mathbb{E} \langle \tilde{\nabla}_k - \nabla f(\mathbf{x}_k), \nabla f(\mathbf{x}_k) \rangle u_{114} + \mathbb{E} \|\mathbf{v}_k\|_2^2 u_{113} + \mathbb{E} \|\nabla f(\mathbf{x}_k)\|_2^2 u_{109} \\
&\quad + \mathbb{E} \|\tilde{\nabla}_k - \nabla f(\mathbf{x}_k)\|_2^2 u_{109} + du_{105} \\
&\leq \mathbb{E} \langle \tilde{\nabla}_k - \nabla f(\mathbf{x}_k), \mathbf{v}_k \rangle u_{111} + \mathbb{E} \|\mathbf{v}_k\|_2^2 u_{123} + \mathbb{E} \|\nabla f(\mathbf{x}_k)\|_2^2 u_{120} \\
&\quad + \mathbb{E} \|\tilde{\nabla}_k - \nabla f(\mathbf{x}_k)\|_2^2 u_{118} + du_{105} \\
&\leq \mathbb{E} \langle \tilde{\nabla}_k - \nabla f(\mathbf{x}_k), \mathbf{v}_k \rangle u_{111} + \mathbb{E} \|\mathbf{v}_k\|_2^2 u_{123} + \mathbb{E} \|\mathbf{x}_k\|_2^2 u_{124} \\
&\quad + \mathbb{E} \|\tilde{\nabla}_k - \nabla f(\mathbf{x}_k)\|_2^2 u_{118} + du_{105} \\
&\leq \mathbb{E} \|\mathbf{v}_k\|_2^2 u_{127} + \mathbb{E} \|\mathbf{x}_k\|_2^2 u_{124} + \mathbb{E} \|\tilde{\nabla}_k - \nabla f(\mathbf{x}_k)\|_2^2 u_{126} + du_{105}
\end{aligned} \tag{55}$$

The first inequality comes from Young's inequalities.

$$\begin{aligned}
\mathbb{E} \langle \nabla f(\mathbf{x}_k), \mathbf{v}_k \rangle &\leq \frac{L \mathbb{E} \|\mathbf{v}_k\|_2^2}{4} + \frac{\mathbb{E} \|\nabla f(\mathbf{x}_k)\|_2^2}{L} \\
\mathbb{E} \langle \tilde{\nabla}_k - \nabla f(\mathbf{x}_k), \nabla f(\mathbf{x}_k) \rangle &\leq \frac{\delta \mathbb{E} \|\nabla f(\mathbf{x}_k)\|_2^2}{2} + \frac{\mathbb{E} \|\tilde{\nabla}_k - \nabla f(\mathbf{x}_k)\|_2^2}{2\delta}
\end{aligned}$$

The second inequality comes from Lipschitz condition.

The third inequality comes from Young's inequalities.

$$\mathbb{E} \langle \tilde{\nabla}_k - \nabla f(\mathbf{x}_k), \mathbf{v}_k \rangle \leq \frac{L \mathbb{E} \|\mathbf{v}_k\|_2^2}{2} + \frac{\mathbb{E} \|\tilde{\nabla}_k - \nabla f(\mathbf{x}_k)\|_2^2}{2L}$$

□

The full expression of terms u_i is as follows.

$$\begin{aligned}
u_{18} &= \frac{\delta}{10\kappa} - 1 \\
u_{24} &= \frac{\delta}{5L\kappa} - \frac{2}{L} \\
u_{27} &= \frac{\delta}{5\kappa} - 2 \\
u_{32} &= \frac{3\delta}{10\kappa} - 1 \\
u_{33} &= \delta - 3 \\
u_{41} &= 3\delta^2 - 2\delta + 3 \\
u_{42} &= u_{41} e^{2\delta} \\
u_{47} &= \frac{u_{33} e^{-\delta}}{8L^2} + \frac{u_{42} e^{-2\delta}}{16L^2} + \frac{3e^{-2\delta}}{16L^2} \\
u_{49} &= 3\delta - 1
\end{aligned}$$

$$\begin{aligned}
u_{52} &= -\frac{u_{49}}{2L} - \frac{e^{-\delta}}{2L} \\
u_{53} &= -\frac{\delta}{2L} - \frac{1}{2L} + \frac{e^{-\delta}}{2L} \\
u_{54} &= \delta - 1 \\
u_{55} &= u_{54}e^{\delta} \\
u_{56} &= -\frac{u_{55}e^{-\delta}}{2L^2} - \frac{e^{-\delta}}{2L^2} \\
u_{57} &= \delta e^{\delta} - u_{49}e^{2\delta} - 4e^{\delta} + 3 \\
u_{60} &= \frac{u_{57}e^{-2\delta}}{4L} \\
u_{61} &= 3 - e^{-\delta} \\
u_{62} &= 1 + e^{-\delta} \\
u_{63} &= \frac{1}{L} - \frac{e^{-\delta}}{L} \\
u_{64} &= \frac{\delta}{10\kappa} - \frac{1}{4} - \frac{e^{-\delta}}{2} + \frac{3e^{-2\delta}}{4} \\
u_{68} &= \frac{3\delta}{2L} - \frac{1}{4L} + \frac{e^{-2\delta}}{4L} \\
u_{70} &= \frac{3\delta^2}{8L^2} - \frac{3\delta}{4L^2} + \frac{\delta e^{-\delta}}{4L^2} + \frac{7}{8L^2} - \frac{5e^{-\delta}}{4L^2} + \frac{3e^{-2\delta}}{8L^2} \\
u_{71} &= 3\delta^2 e^{2\delta} - 10\delta e^{2\delta} + 2\delta e^{\delta} + 11e^{2\delta} - 14e^{\delta} + 3 \\
u_{72} &= \frac{u_{71}e^{-2\delta}}{16L^2} \\
u_{73} &= -\frac{3\delta}{4L} + \frac{\delta e^{-\delta}}{4L} + \frac{5}{4L} - \frac{2e^{-\delta}}{L} + \frac{3e^{-2\delta}}{4L} \\
u_{77} &= |3\delta^2 e^{2\delta} - 6\delta e^{2\delta} + 2\delta e^{\delta} + 7e^{2\delta} - 10e^{\delta} + 3| \\
u_{78} &= 2\delta u_{33}e^{\delta} + u_{77} \\
u_{80} &= \frac{u_{42}e^{-2\delta}}{16L^2} + \frac{3e^{-2\delta}}{16L^2} + \frac{u_{78}e^{-2\delta}}{16L^2\delta} \\
u_{85} &= |-3\delta e^{2\delta} + \delta e^{\delta} + 5e^{2\delta} - 8e^{\delta} + 3| \\
u_{86} &= \frac{\delta u_{77}e^{-2\delta}}{16L^2} + \frac{u_{71}e^{-2\delta}}{16L^2} + \frac{u_{85}e^{-2\delta}}{4L^2} \\
u_{87} &= \frac{\delta}{10\kappa} + \frac{u_{85}e^{-2\delta}}{16} - \frac{1}{4} - \frac{e^{-\delta}}{2} + \frac{3e^{-2\delta}}{4} \\
u_{88} &= L^2 \max(0, u_{86}) \\
u_{89} &= -\frac{7\delta}{10\kappa} + u_{88} \\
u_{90} &= 2|u_{57}| \\
u_{93} &= \frac{\delta\kappa}{2L^2} + \frac{u_{41}}{16L^2} + \frac{u_{90}e^{-2\delta}}{16L^2} + \frac{3e^{-2\delta}}{16L^2} + \frac{u_{78}e^{-2\delta}}{16L^2\delta} \\
u_{96} &= \frac{3\delta}{20\kappa} + \frac{u_{85}e^{-2\delta}}{16} + \frac{u_{90}e^{-2\delta}}{16} - \frac{1}{4} - \frac{e^{-\delta}}{2} + \frac{3e^{-2\delta}}{4} \\
u_{100} &= \frac{10\kappa \max(0, u_{93})}{\delta} \\
u_{101} &= \frac{10\kappa \max(0, u_{96})}{\delta}
\end{aligned}$$

$$\begin{aligned}
u_{102} &= \frac{10\kappa u_{88}}{\delta} \\
u_{104} &= \frac{15\kappa}{L} - \frac{5\kappa}{2L\delta} + \frac{5\kappa e^{-2\delta}}{2L\delta} \\
u_{105} &= \frac{L\delta}{2} - \frac{3L}{4} + Le^{-\delta} - \frac{Le^{-2\delta}}{4} \\
u_{106} &= \delta^2 e^{2\delta} - 2\delta e^{2\delta} + e^{2\delta} \\
u_{107} &= u_{106} + 2u_{55} + 1 \\
u_{108} &= u_{107}e^{-2\delta} \\
u_{109} &= \frac{u_{108}}{16} \\
u_{110} &= \delta e^\delta - u_{54}e^{2\delta} - 2e^\delta + 1 \\
u_{111} &= \frac{Lu_{110}e^{-2\delta}}{4} \\
u_{112} &= e^{2\delta} - 2e^\delta + 1 \\
u_{113} &= \frac{L^2 u_{112}e^{-2\delta}}{4} \\
u_{114} &= \frac{u_{108}}{8} \\
u_{115} &= |u_{107}| \\
u_{116} &= \delta u_{106} + 2\delta u_{55} + u_{115} \\
u_{118} &= \frac{e^{-2\delta}}{16} + \frac{u_{116}e^{-2\delta}}{16\delta} \\
u_{119} &= |u_{110}| \\
u_{120} &= \frac{\delta u_{115}e^{-2\delta}}{16} + \frac{u_{107}e^{-2\delta}}{16} + \frac{u_{119}e^{-2\delta}}{4} \\
u_{121} &= 4e^{2\delta} - 8e^\delta + 4 \\
u_{123} &= \frac{L^2 u_{119}e^{-2\delta}}{16} + \frac{L^2 u_{121}e^{-2\delta}}{16} \\
u_{124} &= L^2 \max(0, u_{120}) \\
u_{125} &= |-\delta e^{2\delta} + \delta e^\delta + u_{112}| \\
u_{126} &= \frac{u_{125}e^{-2\delta}}{8} + \frac{e^{-2\delta}}{16} + \frac{u_{116}e^{-2\delta}}{16\delta} \\
u_{127} &= \frac{L^2 u_{121}e^{-2\delta}}{16} + \frac{3L^2 u_{125}e^{-2\delta}}{16} \\
u_{129} &= 5\delta e^\delta + 5e^{2\delta} \\
u_{132} &= \max \left(0, -\frac{33\kappa}{8} + \frac{3\kappa u_{129}e^{-2\delta}}{8\delta} - \frac{15\kappa e^{-\delta}}{\delta} + \frac{105\kappa e^{-2\delta}}{8\delta}, \right. \\
&\quad \frac{27\kappa}{8} - \frac{\kappa u_{129}e^{-2\delta}}{8\delta} - \frac{5\kappa e^{-\delta}}{\delta} + \frac{45\kappa e^{-2\delta}}{8\delta}, \\
&\quad -\frac{3\kappa}{8} + \frac{5\kappa e^{-\delta}}{8} - \frac{35\kappa}{8\delta} - \frac{5\kappa e^{-\delta}}{\delta} + \frac{75\kappa e^{-2\delta}}{8\delta}, \\
&\quad \left. \frac{57\kappa}{8} - \frac{15\kappa e^{-\delta}}{8} - \frac{55\kappa}{8\delta} + \frac{5\kappa e^{-\delta}}{\delta} + \frac{15\kappa e^{-2\delta}}{8\delta} \right) \\
u_{133} &= \max \left(-\frac{3L^2\delta}{16} + \frac{3L^2\delta e^{-\delta}}{16} + \frac{7L^2}{16} - \frac{7L^2 e^{-\delta}}{8} + \frac{7L^2 e^{-2\delta}}{16}, \right. \\
&\quad \left. \frac{3L^2\delta}{16} - \frac{3L^2\delta e^{-\delta}}{16} + \frac{L^2}{16} - \frac{L^2 e^{-\delta}}{8} + \frac{L^2 e^{-2\delta}}{16} \right)
\end{aligned}$$

$$\begin{aligned}
u_{134} &= \frac{4\kappa^2}{L^2} + \frac{5\kappa}{L^2} \\
u_{135} &= \frac{5u_{134}}{4} \\
u_{137} &= \delta + 2 \\
u_{138} &= \frac{5\kappa u_{137}}{L} \\
u_{146} &= \frac{5u_{134}}{2} \\
u_{147} &= \frac{10\kappa u_{137}}{L} \\
u_{158} &= \frac{25\Theta\delta^4\kappa^3}{L} + \frac{125\Theta\delta^4\kappa^2}{4L} + \frac{150\Theta\delta^3\kappa^3}{L} + \frac{1145\Theta\delta^3\kappa^2}{6L} + \frac{25\Theta\delta^3\kappa}{6L} \\
&\quad + \frac{200\Theta\delta^2\kappa^3}{L} + \frac{250\Theta\delta^2\kappa^2}{L} + \frac{10\delta\kappa}{L} + \frac{20\kappa}{L} \\
u_{159} &= 30\Theta\delta^3\kappa^2 + \frac{75\Theta\delta^3\kappa}{2} + 120\Theta\delta^2\kappa^2 + 150\Theta\delta^2\kappa + 12 \\
u_{160} &= \frac{5L\Theta\delta^4\kappa}{2} + 15L\Theta\delta^3\kappa + \frac{L\Theta\delta^3}{3} + 20L\Theta\delta^2\kappa \\
u_{161} &= 3L^2\Theta\delta^3 + 12L^2\Theta\delta^2
\end{aligned}$$

C Proof of Corollaries 4 to 7

According to Proposition 2-4 in [27], the SAGA gradient estimator satisfies MSEB property with $M_1 = 3N/b^2$, $\rho_M = \frac{b}{2N}$, $M_2 = 0$, $\rho_F = 1$. The SVRG gradient estimator satisfies MSEB property with $M_1 = 3p/b$, $\rho_M = \frac{1}{2p}$, $M_2 = 0$, $\rho_F = 1$. the SARAH gradient estimator satisfies MSEB property with $M_1 = 1$, $\rho_M = 1/p$, $M_2 = 0$, $\rho_F = 1$. the SARGE gradient estimator satisfies MSEB property with $M_1 = 12$, $\rho_M = \frac{b}{2N}$, $M_2 = (27 + 12b)/N$, $\rho_F = \frac{b}{2N}$. Applying these parameters to theorem 1 would lead to corollaries 4 to 7.